

REPORT

**Preliminary Elevated
Temperature Mechanical
Tests in the ETMT**

B Roebuck, M Brooks and M G Gee

July 1998

Preliminary Elevated Temperature Mechanical Tests in the ETMT

B Roebuck, M Brooks and M G Gee
Centre for Materials Measurement & Technology
National Physical Laboratory
Queens Road, Teddington, Middlesex TW11 0LW

ABSTRACT

This report provides the results of preliminary uniaxial strength tests at high homologous temperatures on a number of Ni and steel alloys, obtained in the NPL miniature electro-thermomechanical test system (ETMT). The results are presented as stress versus true strain curves where strain has been measured using a new method based on the variation in resistance that is caused by geometrical changes during deformation.

© Crown copyright 1998
Reproduced by permission of the Controller of HMSO

ISSN 1361-4061

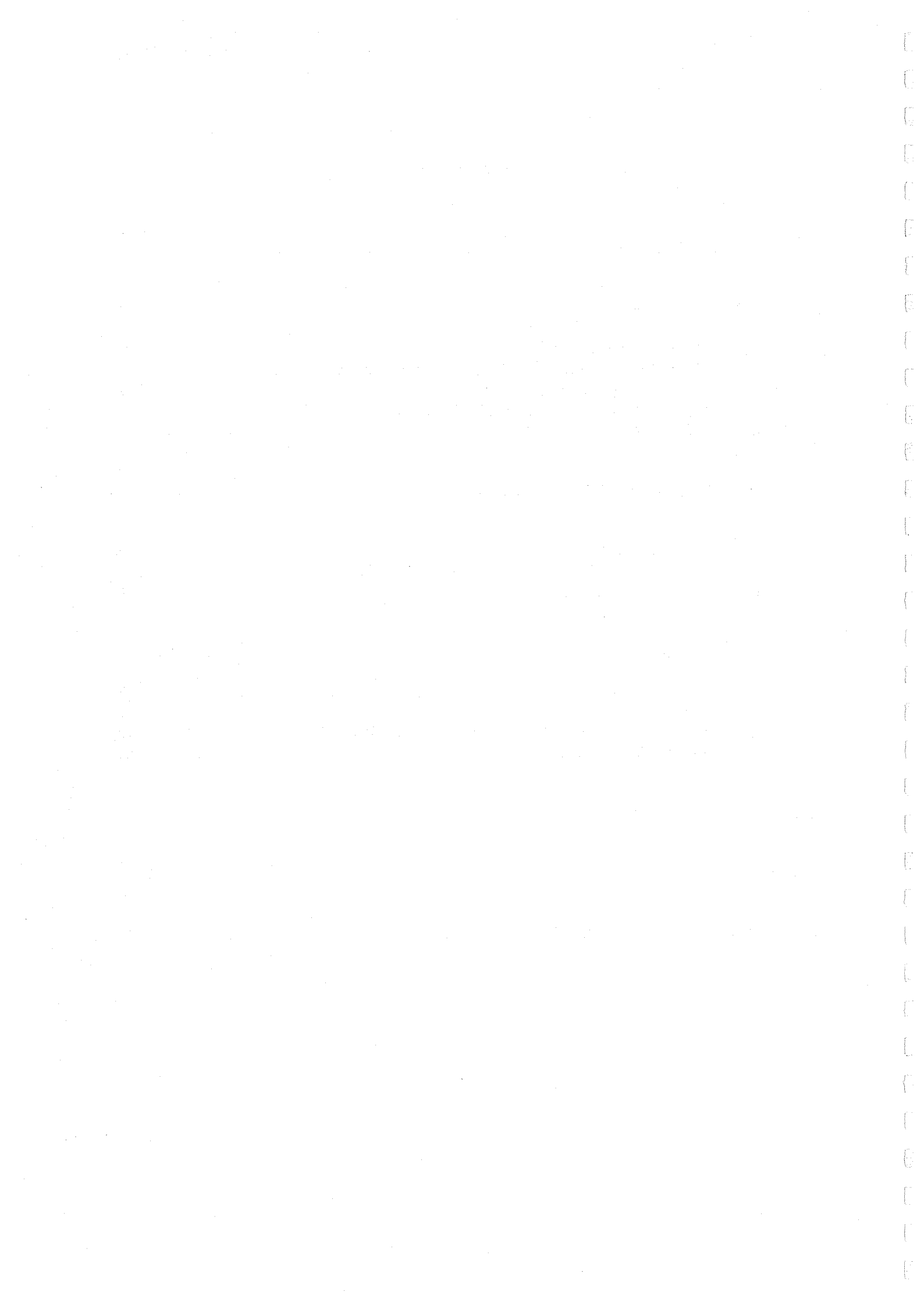
National Physical Laboratory
Teddington, Middlesex, UK, TW11 0LW

Extracts from this report may be reproduced provided the source is
acknowledged.

Approved on behalf of Managing Director, NPL, by Dr C Lea,
Head, Centre for Materials Measurement and Technology

CONTENTS

1	INTRODUCTION	1
2	ETMT	1
	2.1 ETMT SPECIFICATION	1
	2.2 TEMPERATURE MEASUREMENT AND DISTRIBUTION	2
	2.2.1 Temperature Distribution	2
	2.2.2 Thermocouple calibration	4
	2.3 MECHANICAL PROPERTIES	4
3	MATERIALS AND TESTPIECES	6
	3.1 NIMONIC 901	6
	3.2 316 STAINLESS STEEL	6
	3.3 CMSX4 Ni BASE SINGLE CRYSTAL SUPERALLOY	6
	3.4 EUTECTOID STEEL	6
4	TESTS AND RESULTS	7
	4.1 NIMONIC 901	7
	4.2 316 STAINLESS STEEL	7
	4.3 CMSX4 Ni BASE SINGLE CRYSTAL SUPERALLOY	8
	4.4 EUTECTOID STEEL	10
	ACKNOWLEDGEMENTS	11
	LIST OF CAPTIONS	12
	APPENDIX A - Chronology for CMSX4 Tests	14



1 INTRODUCTION

Stress/strain data at high homologous temperatures close to the solidus are required by the metal working and metal casting communities for input into processing models. For Fe and Ni base alloys this presents difficulties because the temperatures of interest lie between 1000-1400 °C. At these high temperatures the measurement of temperature and strain is a technical challenge and no standard methods exist at present. Furthermore, there are problems in gripping testpieces and control of temperature and deformation rate.

As part of project MMP4 - Thermomechanical Behaviour during Metals Processing - NPL is evaluating a miniature test system which can be used to obtain stress/strain data at high homologous temperatures. The system uses DC electric current to heat rectangular cross section testpieces. Strain is measured using changes in electrical resistance by a new technique. This report provides the results of preliminary tests in the ETMT for dissemination to the project industrial advisory group (IAG).

Four materials were tested:

- Nimonic 901
- 316 Stainless Steel
- CSMX4 Ni base single crystal
- Eutectoid Steel

The Nimonic 901 testpieces were manufactured from material supplied for project PMP6. The 316 stainless steel was supplied by Dr P Quedstedt from projects MMP1 and 5. The single crystal material and Eutectoid steel were materials agreed for elevated temperature testing in MMP4.

2 ETMT

The ETMT is a measurement instrument currently being used in the Characterisation of Advanced Materials (CAM) and Measurement for Materials Processing (MMP) Programmes (projects CAM4 and MMP4) of the DTI (EAM Directorate). It has also demonstrated usefulness in project DCC2 of the Design for Composite Components Programme for measurements of the effects of thermal exposure in composite materials.

The ETMT can perform experiments which can be categorised into three types

- Measurement of physical properties
- Measurement of mechanical properties
- Measurement of microstructural stability under thermal exposure.

Testpieces, rectangular (40 x 2 x 1 mm) with a gauge length typically of 10-20 mm, are heated by dc current under computer control to allow the three types of experiment to be conducted as a function of thermal exposure of the testpiece. Both thermal and mechanical loads can be cycled.

2.1 ETMT SPECIFICATION

The ETMT consists of an environmental chamber (500 x 250 x 120 mm) with comprehensive electrical leadthroughs, water cooling and inert gas supply facilities. A computer-controlled DC heating power supply (200A) is used to heat the specimen, with an integral testpiece resistance and thermocouple measurement facility. Testpiece geometries are determined by testpiece resistance. Metallic testpieces, are typically 2 by 1 mm cross section, 40 mm long.

Heating rates up to $200\text{ }^{\circ}\text{C s}^{-1}$ are possible, dependent on the thermal characteristics of the testpiece. Cooling rates are determined by thermal diffusivity of the testpiece and loss of heat to grips. This can typically be $100\text{ }^{\circ}\text{C s}^{-1}$ or $10\text{ }^{\circ}\text{C s}^{-1}$ for good and poor conductors, respectively.

The system uses a mechanical loading assembly ($\pm 1.0\text{ kN}$ maximum), with an in-line or an off-line drive including a flexible testpiece gripping system, a load cell (0.2N resolution) and capacitance displacement transducers (0.4 micrometre resolution); with a computer-controlled motor for null, mean, ramping or fatigue load capability (in or out-of-phase dc current cycle) or constant displacement tests for thermal shock experiments. The motor response is set to about $200\text{-}1000\text{ N s}^{-1}$ for fatigue experiments. Uniaxial tests can have variable (step loading) rates.

The system software uses LabView[®] to monitor and control thermoelectro-mechanical tests and temperature cycles by appropriate feedback control.

The testpiece grips are held at a fixed temperature (room temperature) to provide a constant reference point. This results in parabolic temperature distributions for relatively short testpieces at central temperatures lower than $1100\text{ }^{\circ}\text{C}$. Temperature distributions in testpieces heated to much higher temperatures are not yet known, but are thought to be more uniform in the central parts of the testpiece. More uniform temperatures can be obtained by generating heat at the grips, possibly through the use of higher resistance contacts.

The design of the ETMT is shown schematically in Fig 1.

The results are saved to a text file, which can be opened in for example, Excel[®] or Origin[®], and which consists of:

- Time
- Cycle No.
- Load
- Temperature
- Displacement
- Voltage Drop
- Resistance
- Current

2.2 TEMPERATURE MEASUREMENT AND DISTRIBUTION

2.2.1 Temperature Distribution

Because the testpiece is held in water cooled grips a non-uniform temperature distribution develops along the testpiece. Preliminary examination with a scanning infrared camera of a hot testpiece with a central temperature of about $600\text{ }^{\circ}\text{C}$ indicated that the temperature profile along the testpiece was parabolic. Thus:

$$T(x) = T_m - (T_m - T_G)(x^2/L^2) \quad (1)$$

where $\pm x$ is the distance from the midpoint of the testpiece; where

T_m - the maximum temperature in the centre of the testpiece
 T_G - temperature of grips

and $L = L_T/2$ where L_T is the distance between the positions on the testpiece where the temperature is T_G .

In order to confirm the parabolic distribution, an experiment was planned whereby the resistivity at different points along the testpiece was measured and then, by deducing the temperature/resistivity curve, the temperature at each measurement point could be

calculated. A composite material (a WC/Co hardmetal) was used for this measurement. The testpiece was mounted with a distance of 16.3 mm between the grip faces. Eight Pt wires were spot welded to the testpiece each separated by about 2 mm. The resistivity of the material at room temperature was measured by a 4 probe method and this was used to calibrate the separation distance of each pair of contact wires when in position in the ETMT. The thermocouple was spot welded between the central two contact wires. The sample was then sequentially heated to central temperatures between 100 and 1100 °C in 100 °C steps while monitoring the resistivity of each pair of contact wires. The resistivity data were then plotted against the midpoint of each pair of wires and a second order polynomial was used to fit the data with a regression coefficient of better than 0.99. The resistivity at the position of the thermocouple was then plotted against temperature and the fit of this plot was used to calculate temperature against position. The calculated temperature distributions are shown plotted against position in Fig 2 at 100 °C central temperature intervals, together with a second order polynomial fit. The fit was good (with regression coefficients better than 0.99) thus confirming the parabolic assumption. The temperature range in the central 2 mm of the testpiece was about ± 1 °C at 200 °C, and about ± 2 °C at 400 °C. For higher central temperatures, up to 1100 °C, a parabola was still a reasonable fit, but there was evidence of a more uniform distribution in the centre as might be expected when heat loss by radiation becomes more significant.

Expression (1) can also be used to evaluate variation in testpiece temperature within the central 2 mm of a 20 mm long testpiece beyond central temperatures of 400 °C, as shown in Table 1 below.

**Table 1 - Temperature uniformity with cold grips
(Heat loss dominated by conductivity)**

Central Temperature °C	Temperature ± 1 mm from centre °C	Mean and range (approx) of temperature within central 2 mm
200	198	199 \pm 1
400	396	398 \pm 2
800	792	796 \pm 4

The expression also indicates that for high central temperatures a low variation can be obtained if the grip temperature is raised as shown in Table 2 below.

Table 2 - Temperature uniformity with heated grips

Central Temperature °C	Temperature uncertainty in central 2 mm °C	Required grip temperature °C
800	± 4	20
800	± 2	400
800	± 1	600

These values are for testpieces 20 mm long where it is assumed that the temperature gradient is dominated by thermal conductivity.

More uniform temperatures can also be obtained by testing longer specimens. Table 3 gives an indication of the length of testpiece required to give a temperature variations of ± 1 , ± 2 and ± 4 °C at a central temperature of 800 °C.

Table 3 - Temperature variation with testpiece length

Central Temperature °C	Temperature range in central 2 mm	Testpiece length mm
800	± 4	20
800	± 2	26
800	± 1	40

At higher temperatures radiation losses in the centre become more significant. Therefore further experiments were performed on a Nimonic 901 alloy to examine the temperature distribution along the 16 mm long testpiece at higher temperatures with a central temperature of about 1250 °C. Radiation losses tend to give a more uniform distribution in the centre. It was found that at 1250 °C the variation across the central 2 mm of the testpiece (for a length of 16.3 mm) was ± 1.5 °C (Fig 3). This variation was thought to be acceptable for strength measurements using resistance changes. Longer testpieces should give even more uniform temperatures.

2.2.2 Thermocouple calibration

A further issue is the accuracy of temperature measurement, since thermocouples are made at NPL individually for each test, using 0.1 mm diameter wires of Pt and Pt-13% Rh, that are fusion welded to form a small bead. The bead is then spot welded to the testpiece. Furthermore the voltage is processed by a standard LabView® software routine to give a direct reading in °C. Samples of pure Ti and a eutectoid steel were used to check the combined ETMT software and thermocouple response, since both materials have well defined transformation temperatures. A plot of resistance versus temperature is shown in Fig 4 for pure Ti and normalised resistance versus temperature for the eutectoid steel in Fig 5. Repeat measurements were made and the indicated phase transformation temperatures were with 2-4 °C of each other. The resistance was measured over a 3 mm length in the centre of the testpiece where it is known that the temperature is reasonably uniform. The transformation temperature of the eutectoid steel was confirmed by measurements of the specific heat to be about 740 °C; which agrees well with the resistance measurements.

2.3 MECHANICAL PROPERTIES

The ETMT can be used to perform uniaxial (tension or compression) tests under isothermal temperature conditions. For isothermal conditions the DC heating current is set to a fixed value that ramps the temperature to that close to the required temperature and which is then controlled to maintain the set temperature by incrementing or decrementing the current by a specified amount every 2s. The indicated temperature of the central part of the testpiece is within the range:

$$\begin{array}{ll} \pm 1 \text{ °C up to } 400 \text{ °C} & \pm 2 \text{ °C at } 400 \text{ °C} - 1000 \text{ °C} \\ \pm 5 \text{ °C at } 1000 \text{ °C} - 1500 \text{ °C}. & \end{array}$$

The program maintains control even if the testpiece changes in cross section, providing it is not too fast.

For uniaxial tests the load can be step ramped at rates between 0.05 N/s to 1000 N/s. During the test, changes in length are monitored by the capacitance transducers. The results are plotted as load against displacement. However, it must be noted that the displacement contains an element due to displacement of the rig which is about 0.05 $\mu\text{m}/\text{N}$. Also, if the testpiece is at temperature the displacements measured are an integrated sum of all the deformations occurring along the temperature gradient from centre to grip. A method for obtaining true stress/strain curves from this integrated data has not yet been developed.

Because of the difficulties of deconvoluting the load/displacement data with a temperature distribution, an alternative procedure was developed based on the use of resistance measurements. It was observed that the resistance measured in the central 2-3 mm of the testpiece changed significantly during a deformation test due to a change in the cross sectional area. The resistance increases in tension and decreases in compression. The following analysis was developed to allow true stress/strain data to be obtained from these changes.

The resistance before deformation, R_s , is given by

$$R_s = rL_s/W_sT_s \quad (2)$$

where r is the resistivity, L_s is the length between the contact points for measuring resistance and W_s and T_s are the width and thickness of the testpiece.

At some time t during the test the resistance, R_t , is given by

$$R_t = rL_t/W_tT_t \quad (3)$$

Assuming that the volume, V , remains constant,

$$V_s = V_t = L_sW_sT_s = L_tW_tT_t \quad (4)$$

Thus

$$R_s/R_t = L_s^2/L_t^2 \quad (5)$$

Consequently

$$R_s/R_t = L_s^2/L_t^2 \quad (6)$$

But since true strain, ϵ , is given by

$$\epsilon = \ln (L_t/L_s) \quad (7)$$

then

$$\epsilon = \ln \sqrt{(R_t/R_s)} \quad (8)$$

which is a single expression allowing strain to be calculated as a function of the measured change in resistance.

Examples of the change in resistance during deformation of a Nimonic 901 alloy at high temperature are given in Fig 6 and calculated stress/strain curves in Fig 7.

3 MATERIALS AND TESTPIECES

For all the materials ETMT testpieces were EDM machined, from the material stock, with dimensions of 40 x 2 x 1 mm. Targets, (0.1 thick and 2 mm long), for resistance contacts, were formed integral with the testpiece, separated by 2 mm at one side of the centre of the testpiece, Fig 6.

3.1 NIMONIC 901

Material for test was taken from the 15 mm diameter rod used at NPL for interlaboratory tests in project PMP6 (see NPL report CMMT(A)28, July 1996 on interlaboratory testing).

3.2 316 STAINLESS STEEL

Material for test was taken from a 12 mm diameter rod provided by Dr P Queded, as used in projects MMP1 and 5 on physical property test methods.

3.3 CMSX4 Ni BASE SINGLE CRYSTAL SUPERALLOY

Four CMSX4 rods, 12 mm in diameter and about 200 mm long, were supplied to NPL. The following codes refer to testpieces from each of the rods.

Table 3 - CMSX4 codes

Rod code (Rolls Royce)	ETMT testpiece codes
VFV 1	CMSX4g, CMSX4h, CMSX4i
VFV 4	CMSX4a, CMSX4b, CMSX4c
VFV 7	CMSX4d, CMSX4e, CMSX4f
VFV 8	CMSX4j, CMSX4k, CMSX4l

The room temperature resistivity of testpieces taken from each of the rods was measured in a four probe constant dc current test system (not the ETMT) and the results are shown in Fig 9. The testpieces from rods VFV4, VFV7 and VFV8 were reasonably consistent with less than 1% variation in room temperature resistivity. However, the testpieces taken from rod VFV1 showed more scatter, indicating rather more variability in structure.

3.4 EUTECTOID STEEL

Material for test was taken from a nominally fully pearlitic 6 mm diameter rod supplied by Dr P Morris, British Steel, Swinden Technology Centre, Rotherham. The composition is

0.83% C	0.001% Al
0.26% Si	0.03% N
0.66% Mn	

The room temperature resistivity of six ETMT testpieces were measured using the four probe constant dc current system. All the testpieces gave approximately the same value of resistivity - $1370 \pm 10 \text{ n}\Omega\text{m}$.

4 TESTS AND RESULTS

4.1 NIMONIC 901

A Nimonic 901 testpiece was heated in sequence, firstly to 1100, then 1200 and finally 1300 °C. At each temperature a load was applied at a rate of 2 N/s. This was applied in compression firstly, until the resistance had decreased by about 10%, corresponding to a strain of about 5%. The load was removed quickly and then reapplied in tension at 2 N/s by the same amount, before unloading quickly. The load displacement curves are shown in Fig 10. The corresponding resistance changes were shown in Fig 7 and converted to stress/strain curves in Fig 8.

The flow stress values at 0.5% strain at each test temperature are given in Table 4.1.1.

Table 4.1.1 - Nimonic 901 Flow stress at 0.5% strain, MPa

Temperature °C	Tension	Compression
1000	84	89
1100	31	37
1200	17	17
1300	3	3

A further testpiece was similarly tested at 2 N/s at 1000 °C, but taken to higher deformational strains. The stress/strain curve is shown in Fig 11 and the flow stress data is also included in Table 4.1.1.

4.2 316 STAINLESS STEEL

A 316 stainless steel testpiece was heated, in sequence, firstly to 1100, then 1200 and finally 1300 °C. At each temperature a load was applied at a rate of 2 N/s, as for the Nimonic 901 samples, ie first in compression then in tension. The load/displacement curves are shown in Fig 12, the resistance changes in Fig 13 and the stress/strain curves calculated from the resistance changes in Fig 14.

The flow stress values at 0.5% strain at each temperature are given in Table 4.2.1 and compared with the Nimonic 901 data in Fig 15.

Table 4.2.1 - 316 Stainless Steel Flow Stress at 0.5% strain, MPa

Temperature °C	Tension	Compression
1100	25	27
1200	17	16
1300	11	12

An indication of how quickly samples can be heated to the test temperature is shown in Fig 16 for a stainless steel testpiece heated to 1300 °C in about 10 s.

4.3 CMSX4 Ni BASE SINGLE CRYSTAL SUPERALLOY

A chronological list of the tests performed on the CMSX4 material is given in Appendix A.

The following tables give the results of the tests together with some of the test conditions

Table 1	Load application rates
Table 2	Flow stress at 0.5% strain
Table 3	Flow stress at 1.0% strain
Table 4	Flow stress at different load application rates at 1200 °C

Table 4.3.1 - Load application rates; N/s

Test temperature °C	CMSX4a		CMSX4g		CMSX4d		CMSX4h	
	σ_C	σ_T	σ_C	σ_T	σ_C	σ_T	σ_C	σ_T
1100	2	2	2	2	2	2	-	-
1200	2	2	2	2	2	2	-	-
1150	2	2	2	2	2	2	-	-
1250	2	2	1	1	1	1	-	-
1225	2	2	1	1	1	1	-	-
1275	0.5	0.5	0.5	0.5	1	1	-	-
1300	-	-	-	-	-	-	0.5	0.5

Table 4.3.2 - CMSX4 Flow stress at 0.5% true strain, MPa

Test temperature °C	CMSX4a		CMSX4g		CMSX4d		CMSX4h	
	σ_C	σ_T	σ_C	σ^T	σ_C	σ_T	σ_C	σ_T
1100	185	140	147	128	191	140	-	-
1200	85	73	60	59	77	68	-	-
1150	142	115	115	91	119	102	-	-
1250	24	20	18	23	31	28	-	-
1225	27	24	27	30	58	48	-	-
1275	8.5	8.5	8	15	19	18	-	-
1300	-	-	-	-	-	-	16	12.5

Table 4.3.3 - CMSX4 Flow stress at 1.0% true strain, MPa

Test temperature °C	CMSX4a		CMSX4g		CMSX4d		CMSX4h	
	σ_C	σ_T	σ_C	σ_T	σ_C	σ_T	σ_C	σ_T
1100	243	204	219	202	265	219	-	-
1200	100	88	73	77	101	95	-	-
1150	158	142	140	126	153	139	-	-
1250	28	26	20	26	38	35	-	-
1225	32	30	30	35	65	57	-	-
1275	11	10	10	17	25	23	-	-
1300	-	-	-	-	-	-	18	15

Table 4.3.4 - CMSX4h - Flow stress (at 0.5 and 1.0% true strain) at different load rates, 1200 °C, MPa

Load Rate, N/s	0.5% strain		1.0% strain	
	σ_C	σ_T	σ_C	σ_T
0.5	67	55	85	72
5	67	63	91	81

CMSX4 Resistance

In assessing the repeatability of mechanical test data at high temperature of materials, it is important that the structure and composition of testpieces are thoroughly characterised. This is especially the case for cast materials. Consequently the resistances of the CMSX4 testpieces were measured during heating to the appropriate test temperature. The results are shown in Figs 17-23 as normalised resistance versus temperature plots. The data is plotted as normalised resistance, ie measured resistance divided by the resistance at 400 °C. This is because, in the ETMT, the resistance at room temperature is measured with a small current of about 1 A and the signal is noisier than it is at 400 °C. Also, after each cycle of heating, there were small differences in testpiece dimensions, hence a normalised plot enables easier comparisons to be made between different temperature cycles.

Figs 17-20 show the normalised resistance data for tests where the testpieces were heated in one run to two temperatures, i.e. 1100 °C and 1200 °C, 1150 °C and 1250 °C and 1225 °C and 1275 °C. The plot in black corresponds to the first cycle. For each testpiece the first cycle differed slightly from subsequent cycles, which then remained similar. The reason for this is not known.

The vertical lines on each plot correspond to where the resistance changed when compression and tension loads were applied to the testpiece.

Figs 20-23 show plots in green where the testpieces were heated to the solidus. At the solidus the resistance increases due to the formation of liquid with a much higher resistance

than the solid. Figs 22 and 23 show expanded plots of Figs 20 and 21 with a solidus temperature of about 1355 °C measured for two testpieces CMSX4d5 and CMSX4h4. Clearly the measurement of resistance will be useful in performing mechanical tests at temperatures above the solidus.

Also interesting to note in Figs 22 and 23 are two peaks in the resistance/temperature plots just prior to the solidus. These are clearer to see in Fig 23 where the heating rate was slower than that in Fig 22. It is not known what microstructural changes cause these peaks.

CMSX4 Stress/Strain Data

Stress/strain plots obtained from changes in resistance are shown in Figs 24-33. These measurements were obtained in the sequences shown in Appendix A, where testpieces were deformed in compression and then in tension at one temperature, then heated to the second (higher) temperature and again tested in compression and tension. It is not known at this stage whether there is an effect of testing history on the flow stress data.

Also, some of the tests were performed at different loading rates. This will have an effect on flow stress as can clearly be seen in Fig 34 which shows flow stress data at 1200 °C in tension and compression for loading rates differing by a factor of 10 on a testpiece (CMSX4h2) from rod VFV1.

Flow stress values at 0.5% and 1.0% true strain from the data shown in Figs 24-34 are plotted in Figs 35-38. The tension and compression data have been separated and there is a clear trend of higher flow stress values in compression than in tension, as found for tests on the Nimonic 901 and 316 stainless steel (Fig 15).

The results in Figs 35-38 show some scatter, but this is consistent with the scatter in composition indicated by the resistivity measurements on rod VFV1.

The CMSX4 compression flow stresses at 0.5% strain from testpiece CMSX4d are shown compared with the Nimonic 901 and 316 stainless steel results in Fig 39.

4.4 EUTECTOID STEEL

Only two tests have been performed on the eutectoid steel to date because in the first experiments some difficulty was experienced with oxidation of the testpiece at temperatures greater than 1200 °C even though the tests were performed in flowing argon.

The testpieces were coded eusta4 and eustb2. Plots of the change in normalised resistance (normalised to the value at 400 °C for the same reason as tests on the CMSX4 single crystal Ni alloy) are shown in Fig 5. The transformation at an indicated temperature of 740-745 °C can clearly be seen. The samples were not heated to the solidus because of the oxidation problem. At 1250 °C the samples were oxidising at a rate equivalent to a loss of metal at a rate of 0.15 µm/s. This corresponded to a change in resistance from 1.500 milliohms to 1.515 milliohms in a period of 40 s.

The first testpiece, eusta4 was heated to 1100 °C and deformed in compression at 2.5 N/s. The second testpiece was heated to 1250 °C and deformed in compression and then tension at 0.5 N/s. Only the compression data was calculated from the change in resistance. The calculated stress/strain data are shown in Fig 40. The data at 1250 °C are shown both uncorrected and corrected for the resistance change due to oxidation. The testpieces appear to go into tension because the resistance is increasing due to oxidation superimposed on the decrease due to deformation. The oxidation increase was linear and was thus straightforward to correct.

The flow stress data at 0.5% and 1.0% strain are given in Table 4.4.1.

**Table 4.4.1 - Eutectoid steel flow stresses
at 0.5% and 1.0% strain in compression, MPa**

Temperature °C	Compression Flow Stress	
	0.5% strain	1.0% strain
1100	15.5	18.5
1250	10.5	11.5

The data is also plotted for comparison with that obtained for the Nimonic 901, 316 stainless steel and CSMX4 Ni base single crystal alloy in Fig 39.

ACKNOWLEDGEMENTS

The work performed for this report was supported by the DTI MMP programme within project MMP4 on Thermomechanical Behaviour during Metals Processing.

LIST OF CAPTIONS

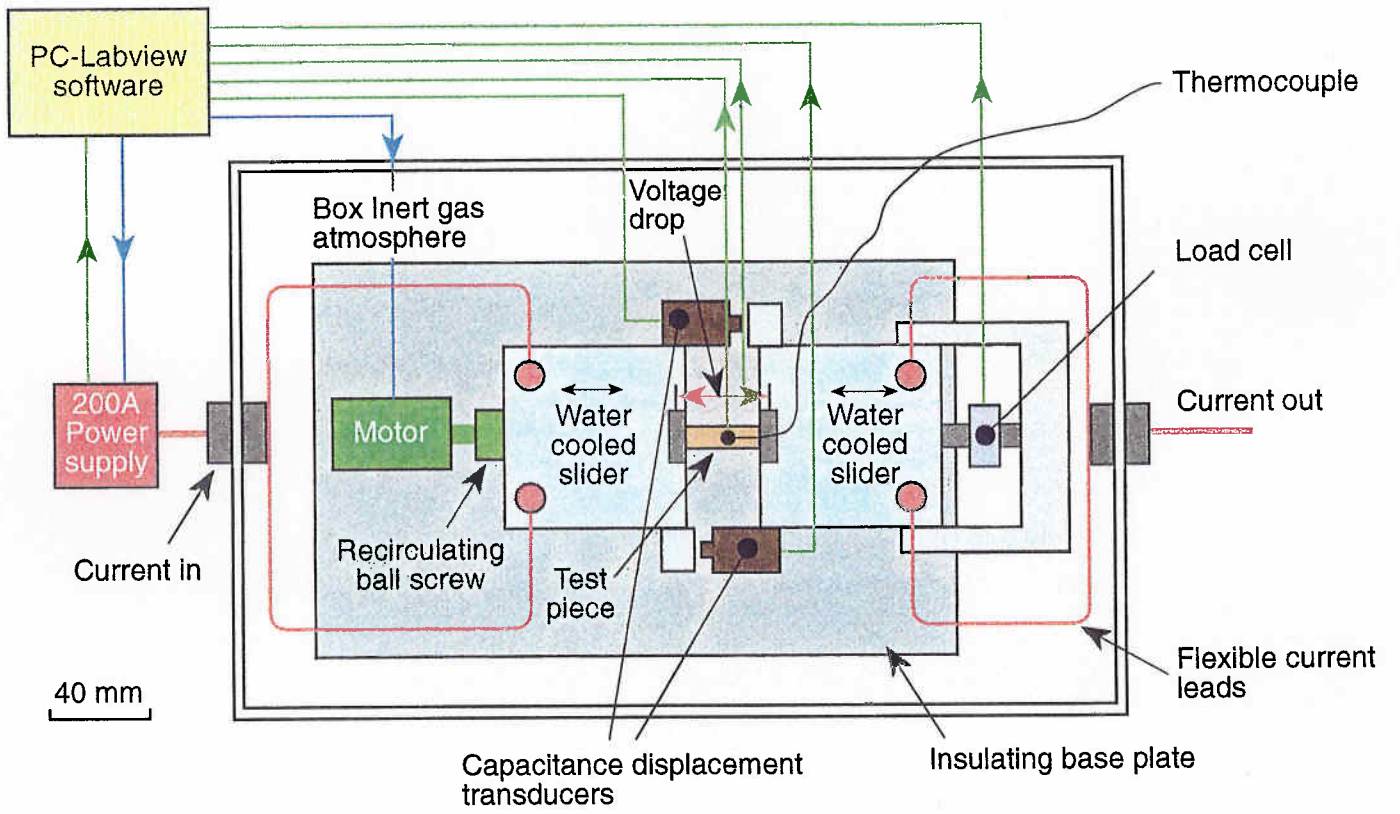
- Fig 1 Schematic diagram of In-line ETMT.
- Fig 2 Parabolic temperature distributions.
- Fig 3 Temperature distribution with a central temperature of 1250 °C.
- Fig 4 Resistance/temperature plot for pure Ti showing phase transformation at about 870 °C.
- Fig 5 Normalised resistance/temperature plot for eutectoid steel showing phase transformation at about 740-745 °C.
- Fig 6 Change in resistance during deformation of a Nimonic 901 alloy.
- Fig 7 Typical stress/strain plots for Nimonic 901 calculated from changes in resistance.
- Fig 8 Schematic diagram of ETMT testpiece showing integral targets for resistance contacts.
- Fig 9 Room temperature resistivity of ETMT testpieces from each of the four CMSX4 bars.
- Fig 10 Load/displacement curves for tests on Nimonic 901.
- Fig 11 Stress/strain curve from Nimonic 901 tested at 1000 °C.
- Fig 12 Load/displacement curves for tests on 316 stainless steel.
- Fig 13 Resistance/temperature plot for 316 stainless steel tested at 1100, 1200 and 1300 °C.
- Fig 14 Stress/strain curves for 316 stainless steel tested at 1100, 1200 and 1300 °C calculated from resistance changes.
- Fig 15 Flow stress data at 0.5% strain for Nimonic 901 and 316 stainless steel in tension and compression.
- Fig 16 Heating rate to 1300 °C for 316 stainless testpiece.
- Fig 17 Normalised resistance/temperature plot for tests on CMSX4a.
- Fig 18 Normalised resistance/temperature plot for tests on CMSX4d.
- Fig 19 Normalised resistance/temperature plot for tests on CMSX4g.
- Fig 20 Normalised resistance/temperature plot for tests on CMSX4h.
- Fig 21 Normalised resistance/temperature plot for tests on CMSX4d, showing heating cycle to solidus.
- Fig 22 Expanded plot of Fig 21 on CMSX4d.
- Fig 23 Expanded plot of Fig 20 on CMSX4h.
- Fig 24 Stress/strain plot in tension and compression at 1150 °C and 1250 °C for CMSX4a2 (rod VFV4).

- Fig 25 Stress/strain plot in tension and compression at 1225 °C and 1275 °C for CMSX4a3 (rod VFV4).
- Fig 26 Stress/strain plot in tension and compression at 1100 °C and 1200 °C for CMSX4a1 (rod VFV4).
- Fig 27 Stress/strain plot in tension and compression at 1100 °C and 1200 °C for CMSX4d2 (rod VFV7).
- Fig 28 Stress/strain plot in tension and compression at 1150 °C and 1250 °C for CMSX4d3 (rod VFV7).
- Fig 29 Stress/strain plot in tension and compression at 1225 °C and 1275 °C for CMSX4d4 (rod VFV7).
- Fig 30 Stress/strain plot in tension and compression at 1100 °C and 1200 °C for CMSX4g1 (rod VFV1).
- Fig 31 Stress/strain plot in tension and compression at 1150 °C and 1250 °C for CMSX4g2 (rod VFV1).
- Fig 32 Stress/strain plot in tension and compression at 1225 °C and 1275 °C for CMSX4g3 (rod VFV1).
- Fig 33 Stress/strain plot in tension and compression at 1300 °C for CMSX4h3 (rod VFV1).
- Fig 34 Stress/strain plots at different loading rates at 1200 °C for CMSX4h2 (rod VFV1).
- Fig 35 Flow stress at 0.5% strain in compression on CMSX4.
- Fig 36 Flow stress at 0.5% strain in tension on CMSX4.
- Fig 37 Flow stress at 1.0% strain in compression on CMSX4.
- Fig 38 Flow stress at 1.0% strain in tension on CMSX4.
- Fig 39 Flow stress at 0.5% strain for tests on Nimonic 901, 316 stainless steel, CMSX4 single crystal Ni alloy and Eutectoid steel.
- Fig 40 Compression stress/strain data for eutectoid steel at 1100 °C and 1250 °C, showing correction for oxidation.

APPENDIX A - Chronology for CMSX4 Tests

Testpiece and file name	Date	Action
CMSX4a1	3/11/97	a) Heated to 1200 °C, tested in compression then tension b) Cooled to 1100 °C, tested in compression then tension c) Cooled to RT, slowly
CMSX4a2	3/11/97	a) Heated to 1250 °C, tested in compression then tension b) Cooled to 1150 °C, tested in compression then tension c) Cooled to RT, slowly
CMSX4a3	3/11/97	a) Heated to 1225 °C, tested in compression then tension b) Cooled to 1275 °C, tested in compression then tension c) Heated to melting, 0 load
CMSX4b1	3/11/97	a) Heated to 1200 °C, tested in compression then tension b) Thermocouple came off during tests
CMSX4g1	23/12/97	a) Heated to 1100 °C, tested in compression then tension b) Heated to 1200 °C, tested in compression then tension c) Cooled to RT, slowly
CMSX4g2	23/12/97	a) Heated to 1150 °C, tested in compression then tension b) Heated to 1250 °C, tested in compression then tension c) Cooled to RT, slowly
CMSX4g3	23/12/97	a) Heated to 1225 °C, tested in compression then tension b) Heated to 1275 °C, tested in compression then tension c) Cooled to RT, slowly
CMSX4g4	23/12/97	a) Measured cooling rate (self quench) from 200 °C
CMSX4g5	23/12/97	a) Loaded at RT to 500 MPa (data not saved!)
CMSX4g6	23/12/97	a) Heated to 950 °C then 500 MPa applied until ruptured (creep)
CMSX4d1	24/12/97	a) Heated to 950 °C, left for about 30 mins to check resistance stability (no change) b) Cooled to RT slowly
CMSX4d2	24/11/97	a) Heated to 1100 °C, tested in compression then tension b) Heated to 1200 °C, tested in compression then tension c) Cooled to RT, slowly
CMSX4d3	24/12/97	a) Heated to 1150 °C, tested in compression then tension b) Heated to 1250 °C, tested in compression then tension c) Cooled to RT, slowly
CMSX4d4	24/12/97	a) Heated to 1225 °C, tested in compression then tension b) Heated to 1275 °C, tested in compression then tension c) Cooled to RT, slowly
CMSX4d5	24/12/97	a) Heated until melted, 0 load

Testpiece and file name	Date	Action
CMSX4h1	12/1/98	a) Heat to 1250 °C and cool to RT, slowly
CMSX4h2	12/1/98	a) Heat to 1200 °C, deform in compression then tension at 0.5 N/s b) Keep at 1200 °C, deform in compression then tension at 5 N/s c) Leave at 1200 °C for 6 min (0 load) to check resistance (no change) d) Cool to RT, slowly
CMSX4h3	13/1/98	a) Heat to 1300 °C, test in compression then tension b) Cool to RT, slowly
CMSX4h4	13/1/98	a) Heat to melting, slowly



Miniature Thermomechanical Test Rig

46593

Fig 1 Schematic diagram of In-line ETMT.

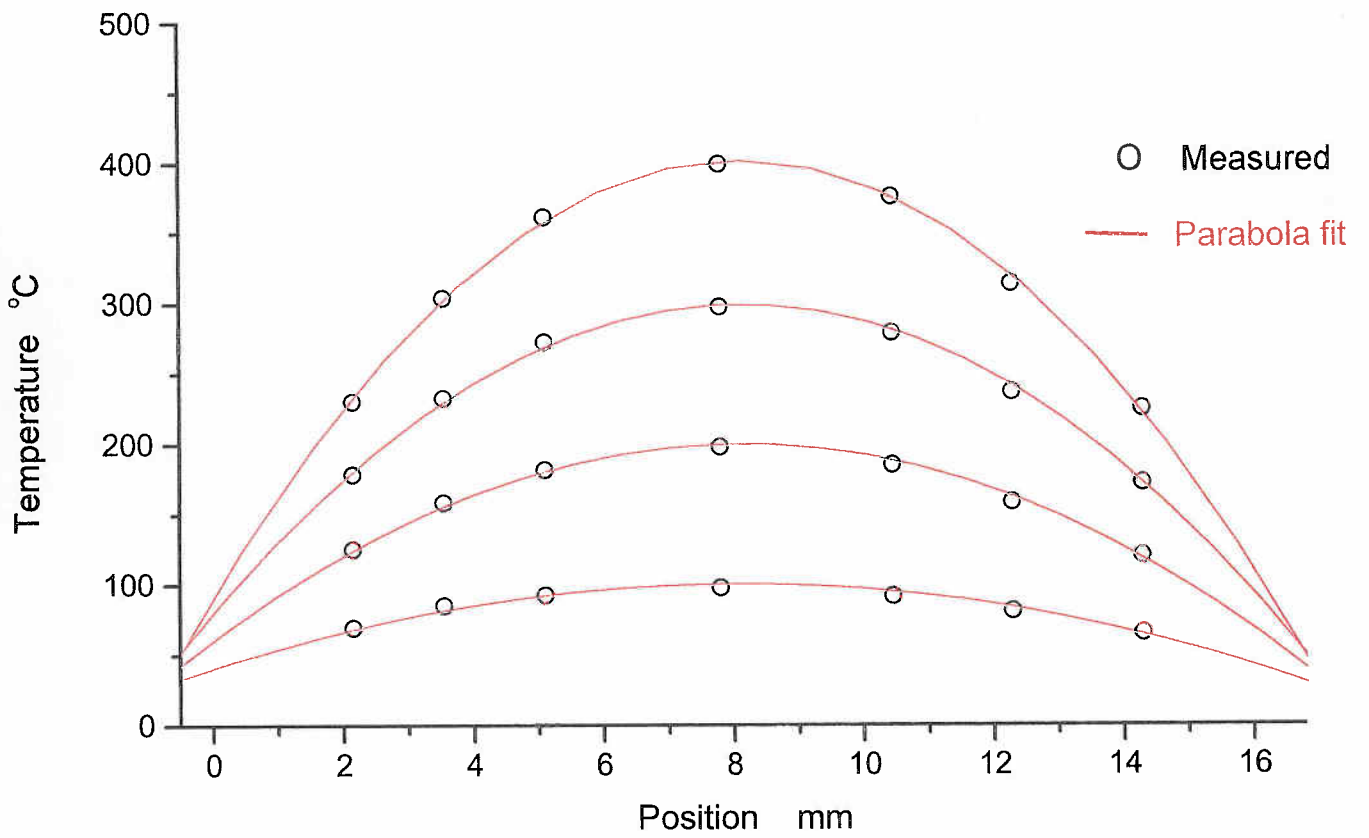


Fig 2 Parabolic temperature distributions.

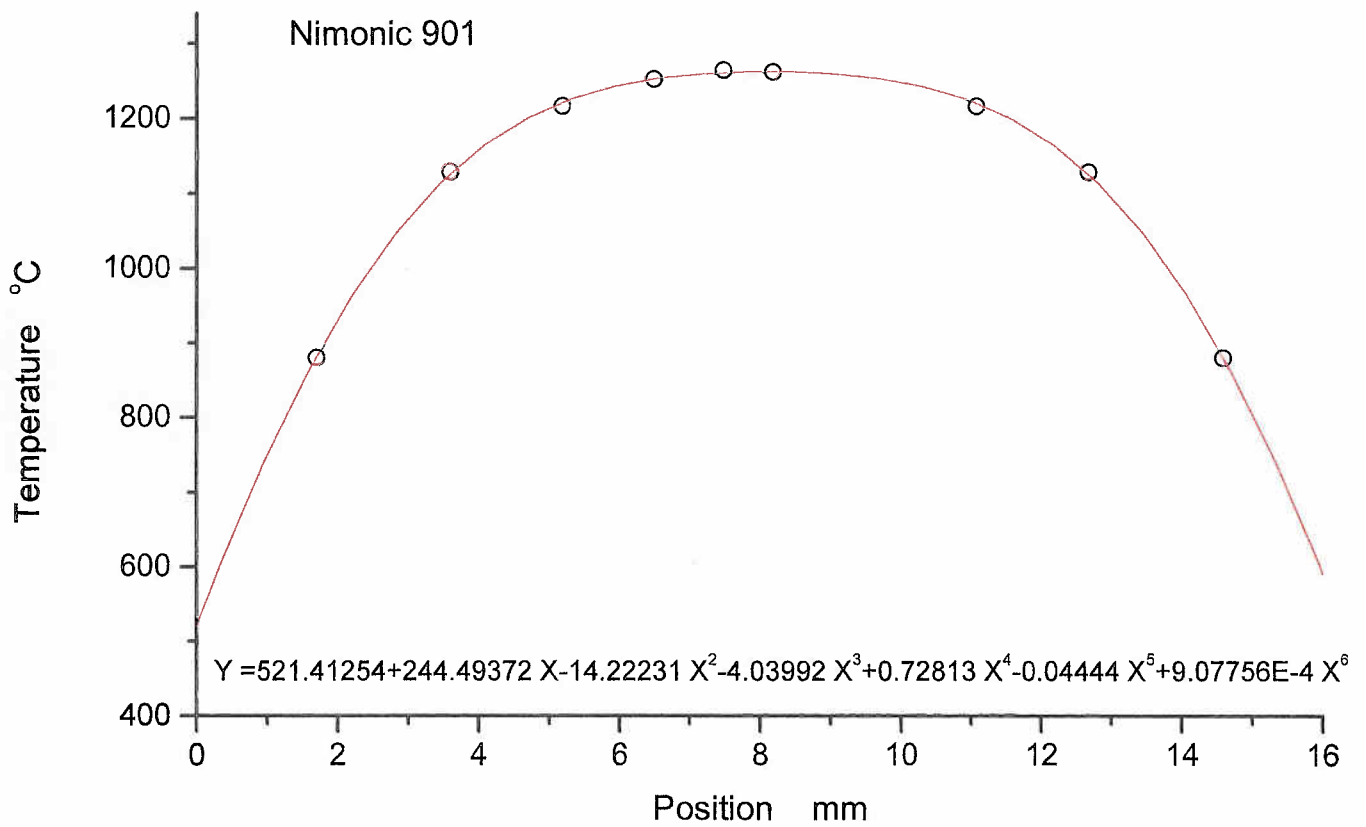


Fig 3 Temperature distribution with a central temperature of 1250 °C.

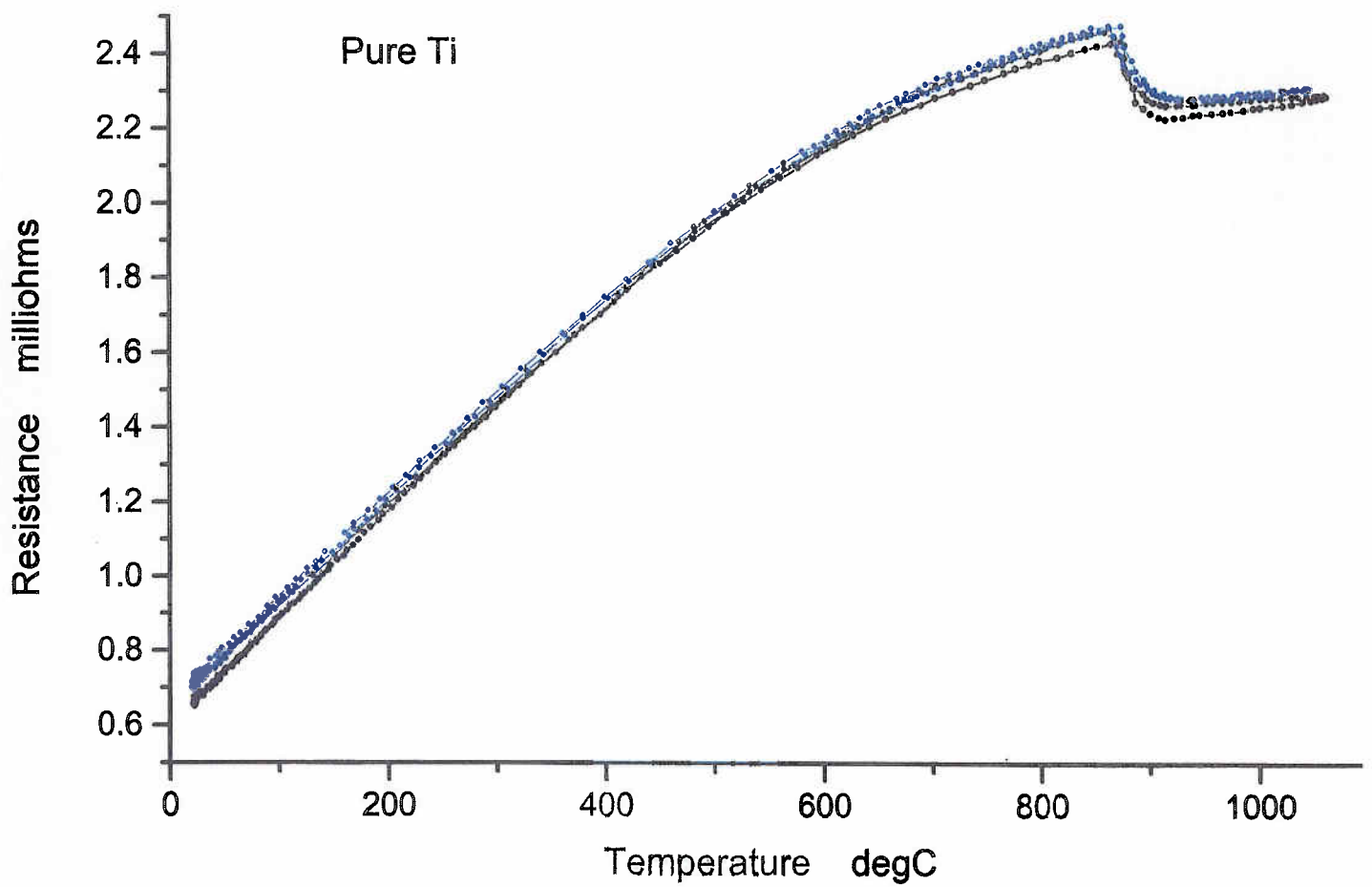


Fig 4 Resistance/temperature plot for pure Ti showing phase transformation at about 870 °C.

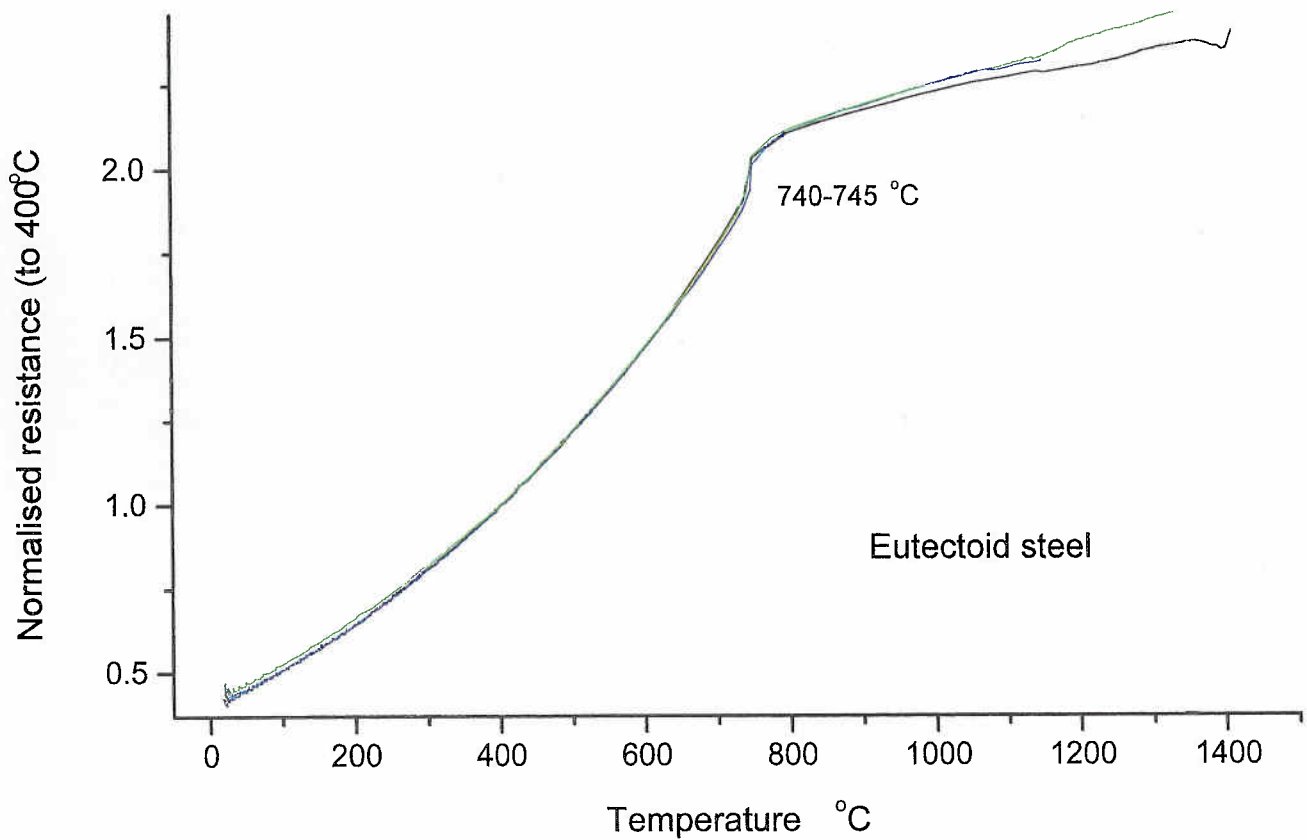


Fig 5 Normalised resistance/temperature plot for eutectoid steel showing phase transformation at about 740-745 °C.

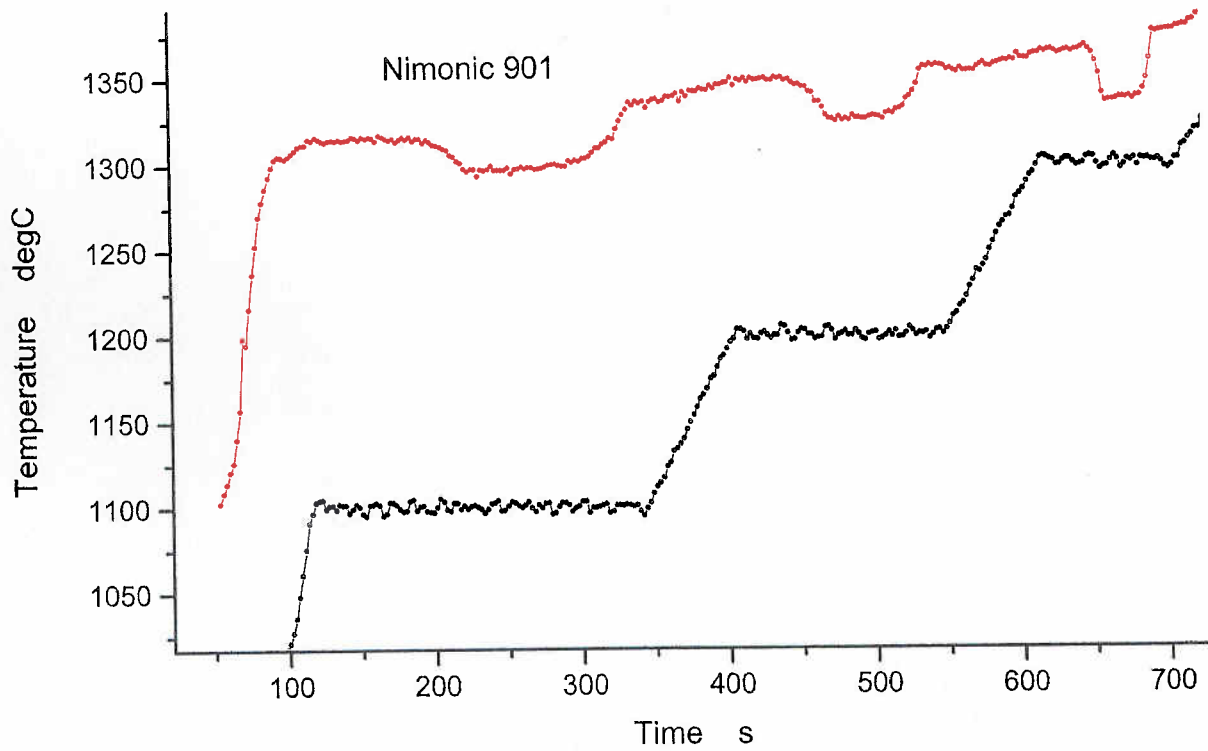


Fig 6 Change in resistance during deformation of a Nimonic 901 alloy.

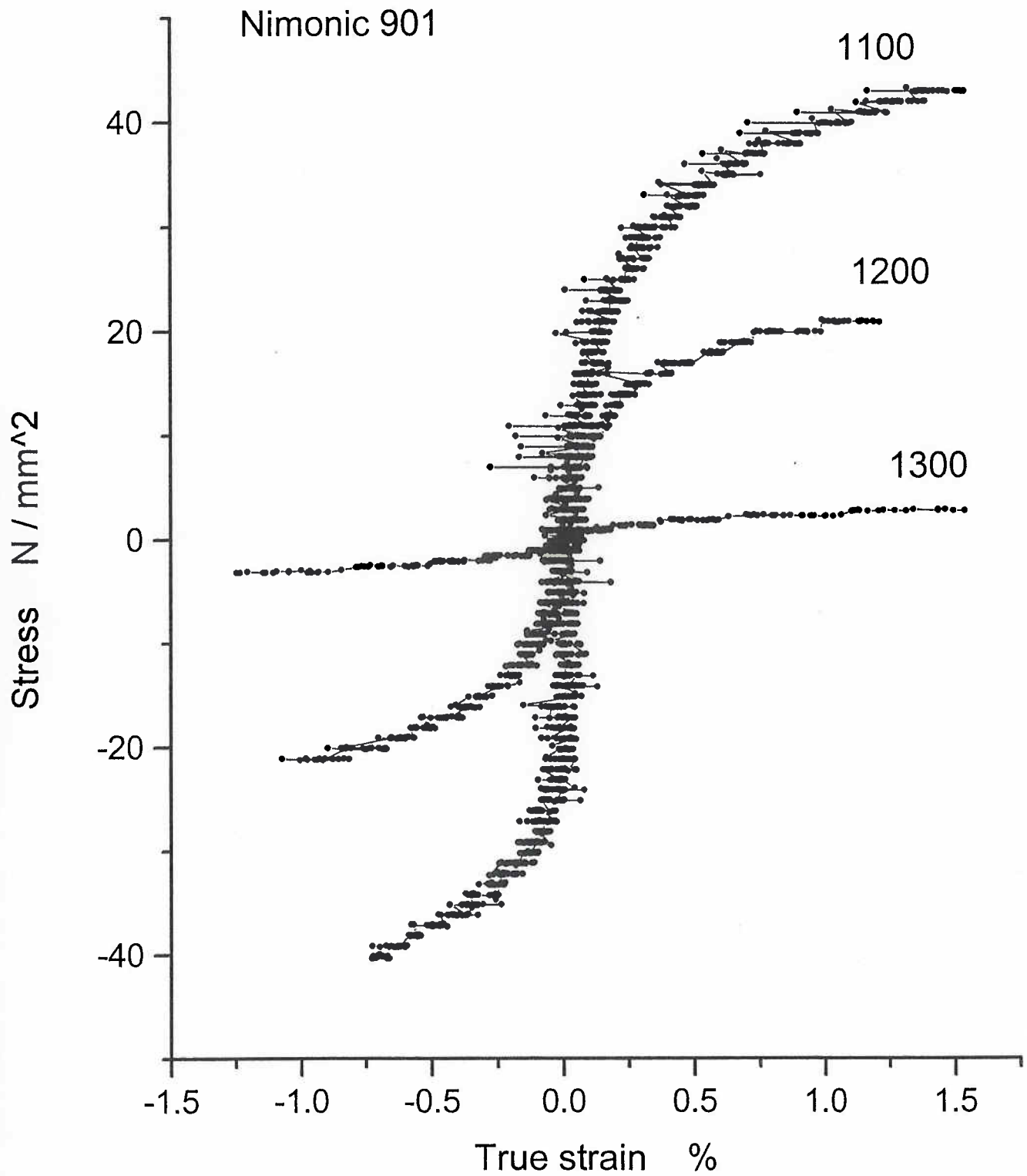
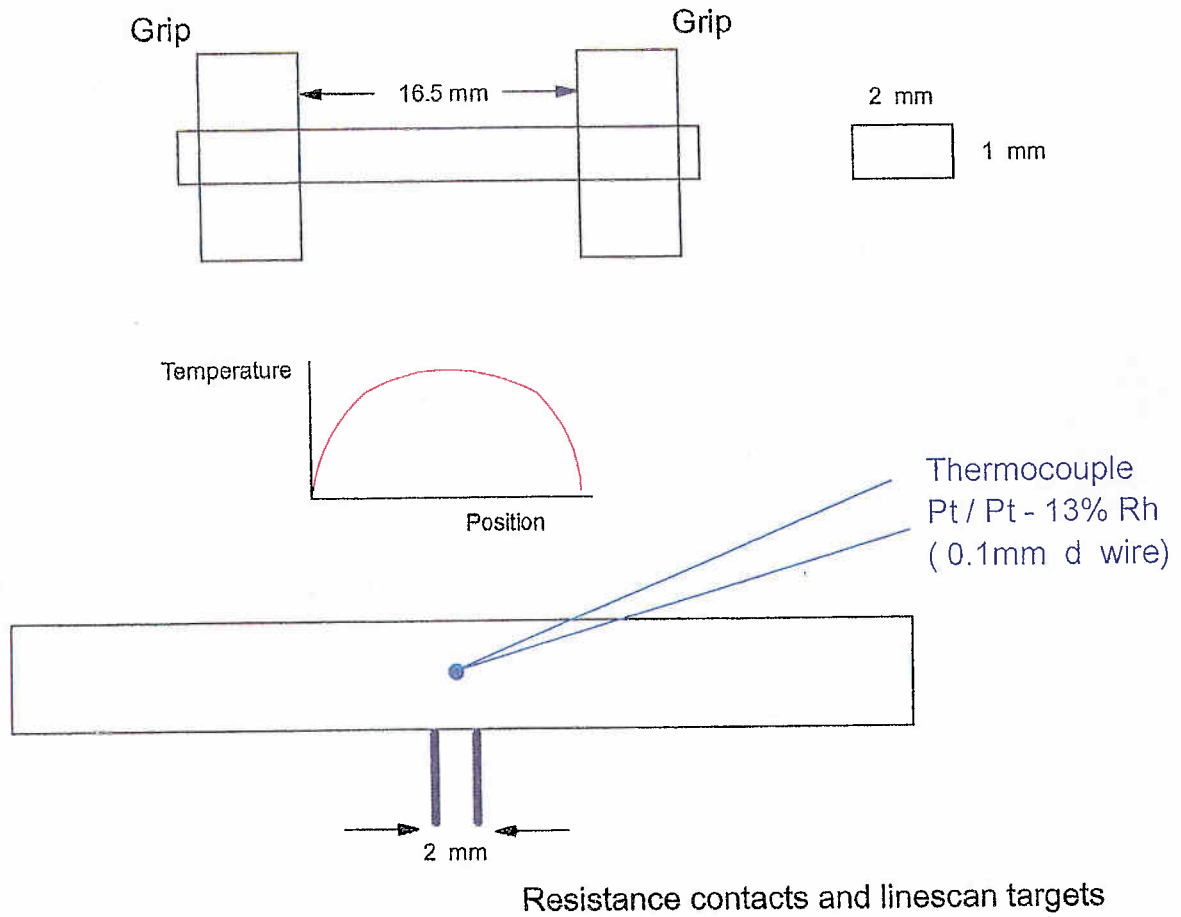


Fig 7 Typical stress/strain plots for Nimonic 901 calculated from changes in resistance.



ETMT testpiece design for High Temperature tests

Fig 8 Schematic diagram of ETMT testpiece showing integral targets for resistance contacts.

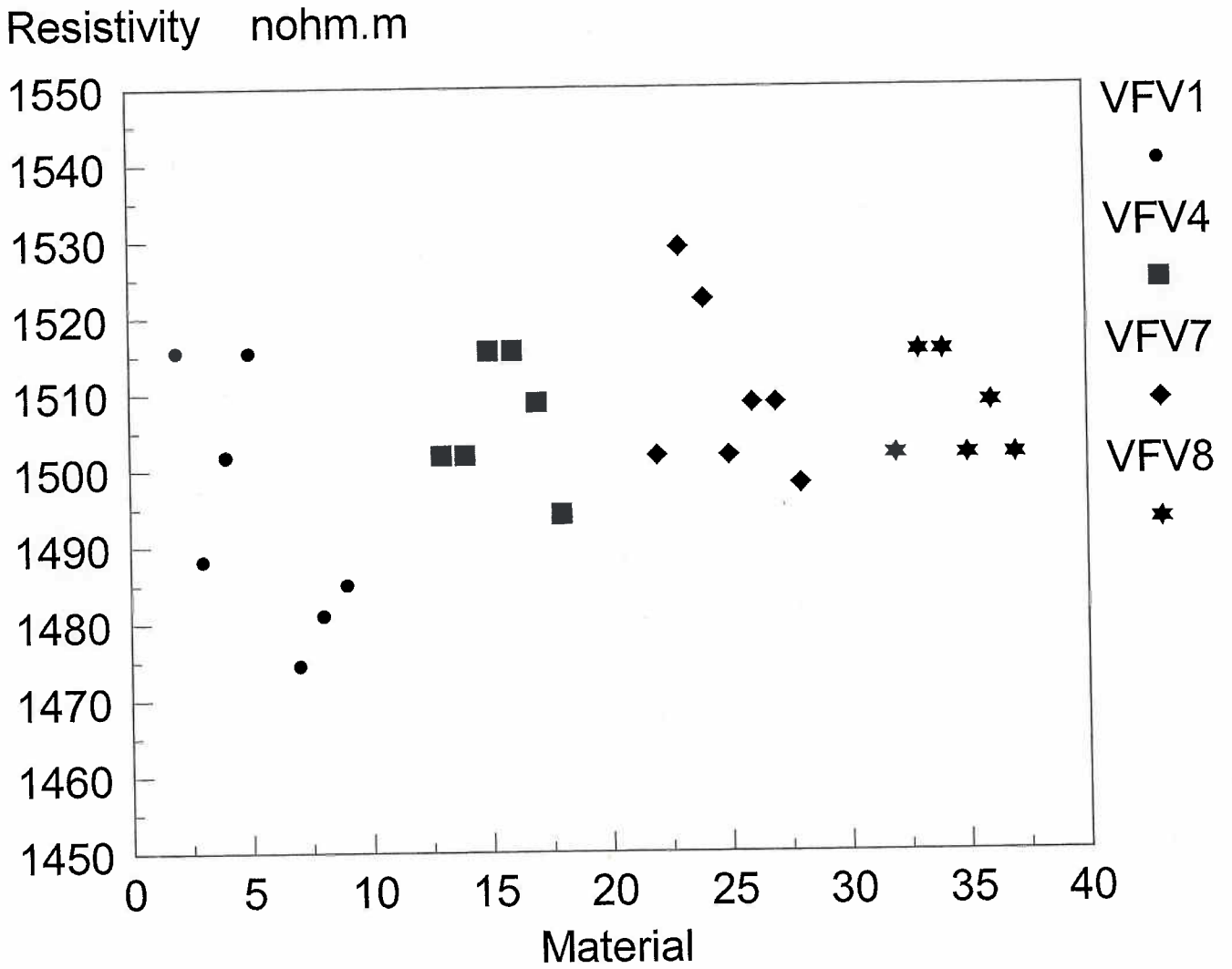


Fig 9 Room temperature resistivity of ETMT testpieces from each of the four CMSX4 bars.

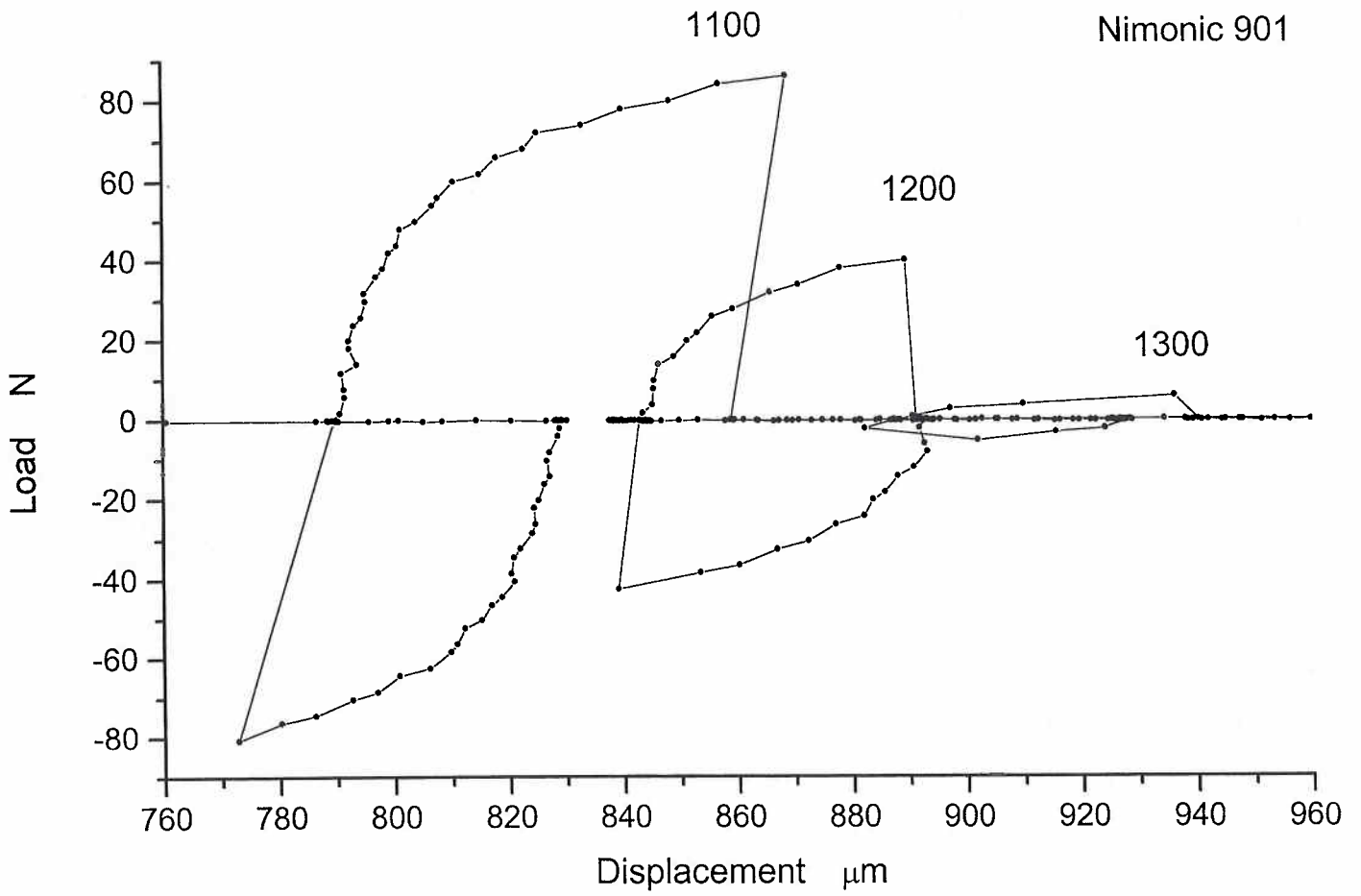


Fig 10 Load/displacement curves for tests on Nimonic 901.

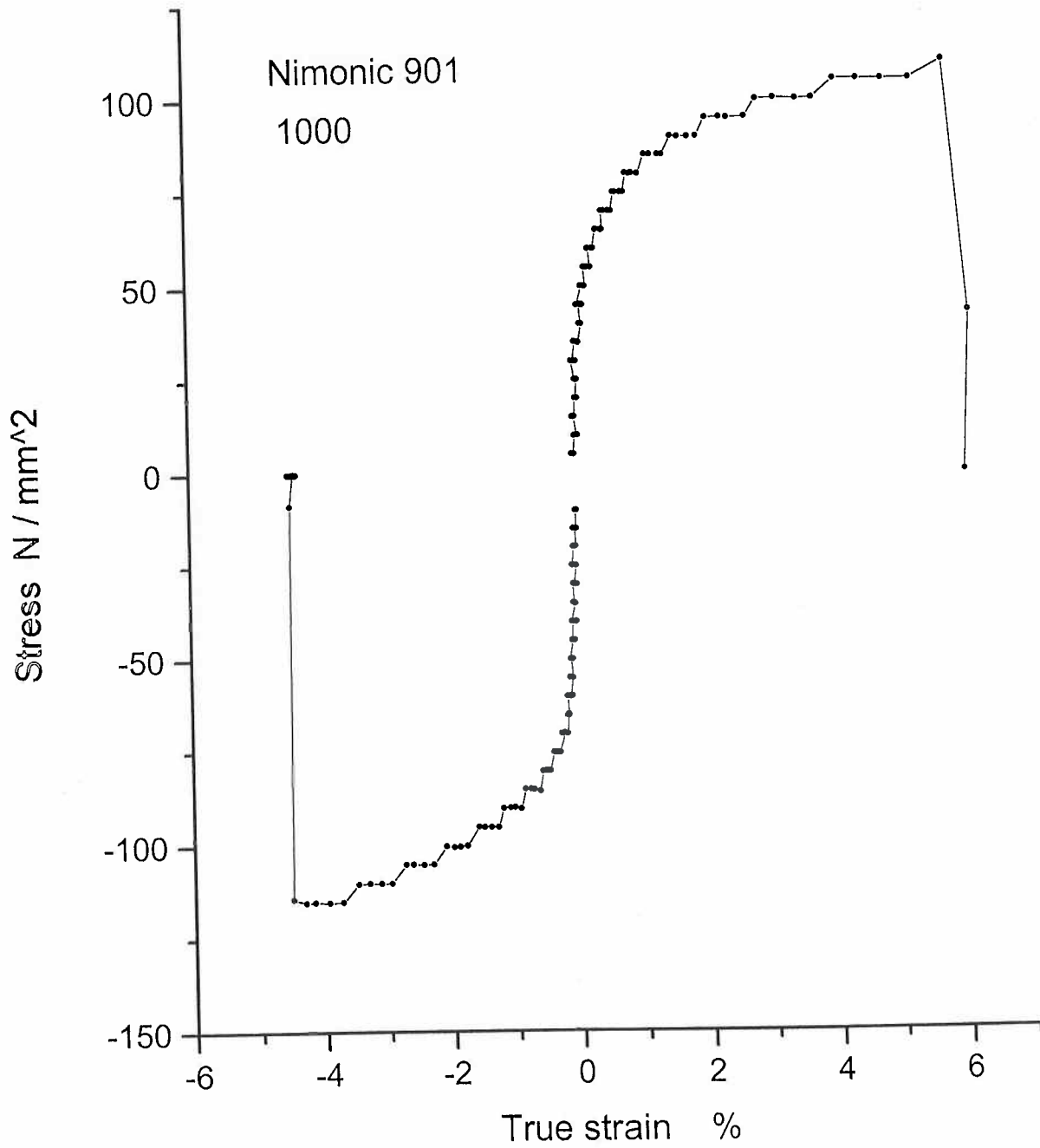


Fig 11 Stress/strain curve from Nimonic 901 tested at 1000 °C.

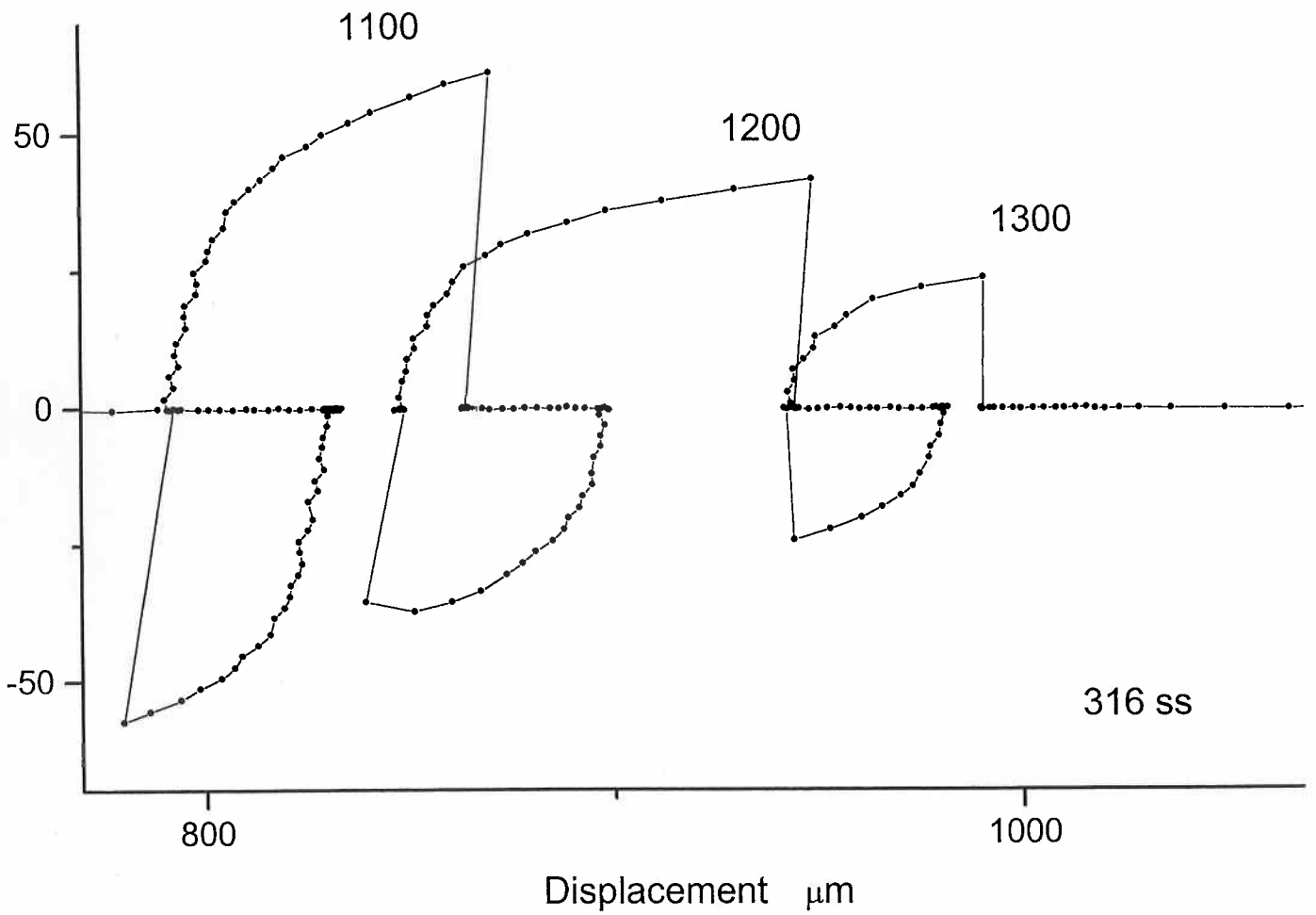


Fig 12 Load/displacement curves for tests on 316 stainless steel.

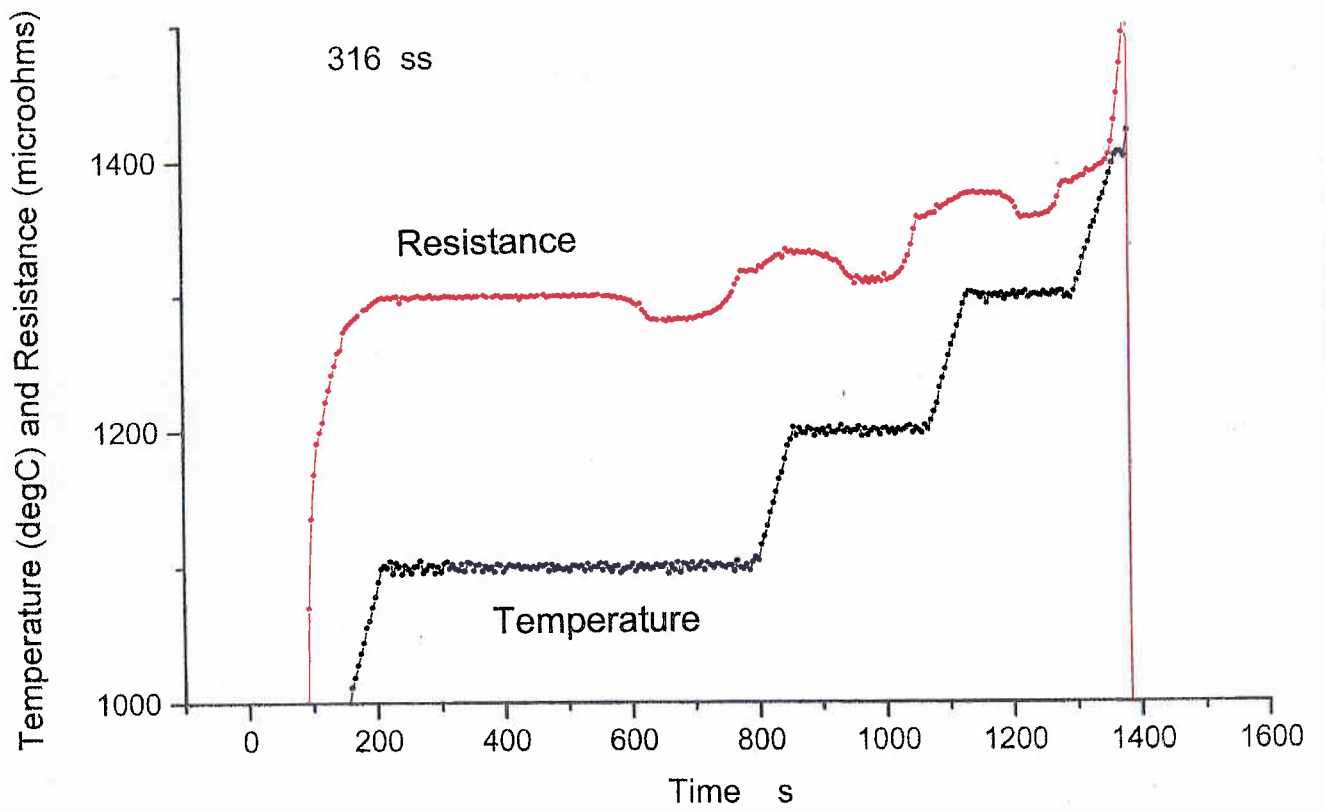


Fig 13 Resistance/temperature plot for 316 stainless steel tested at 1100, 1200 and 1300 °C.

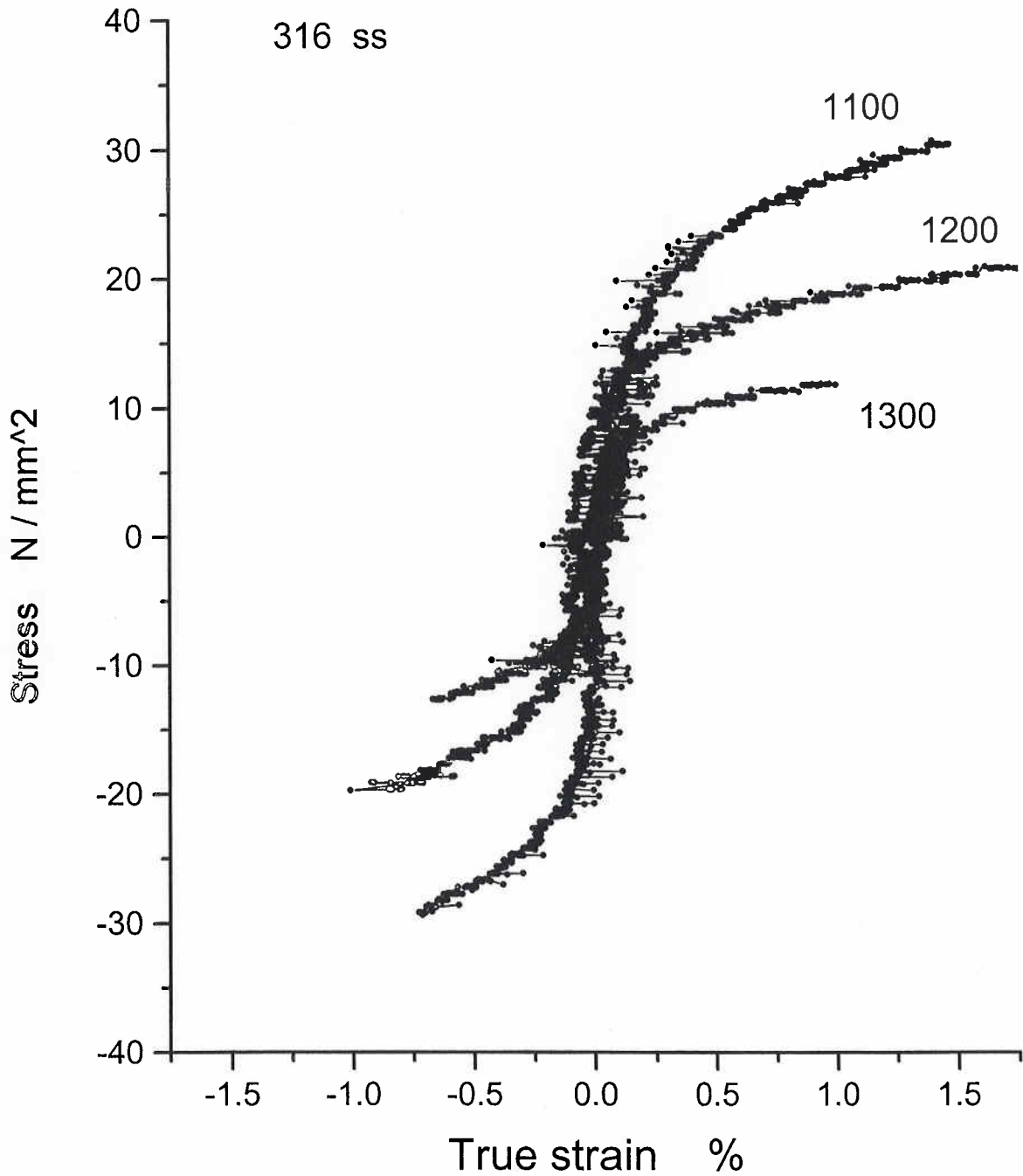


Fig 14 Stress/strain curves for 316 stainless steel tested at 1100, 1200 and 1300 °C calculated from resistance changes.

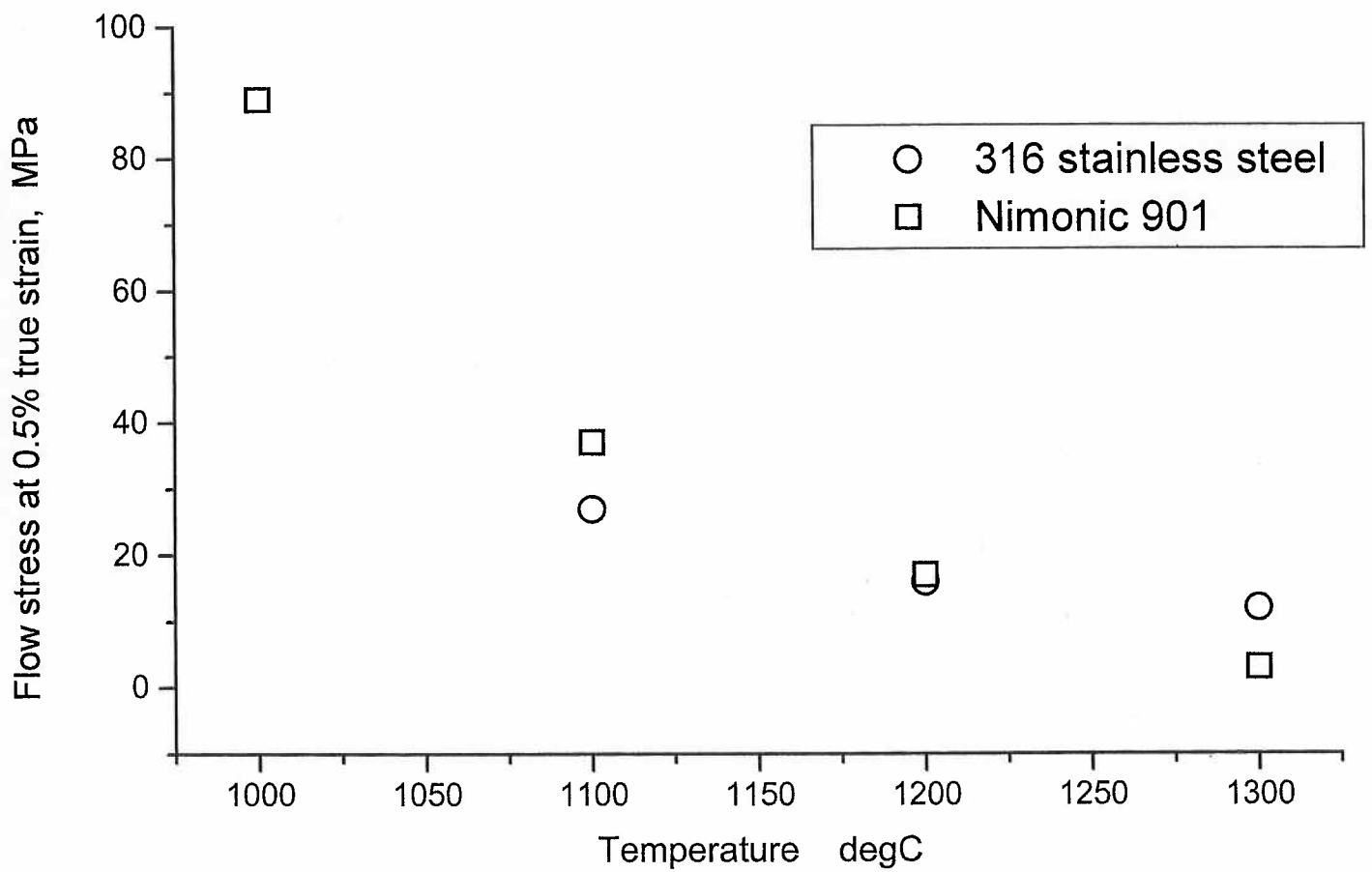


Fig 15 Flow stress data at 0.5% strain for Nimonic 901 and 316 stainless steel in tension and compression.

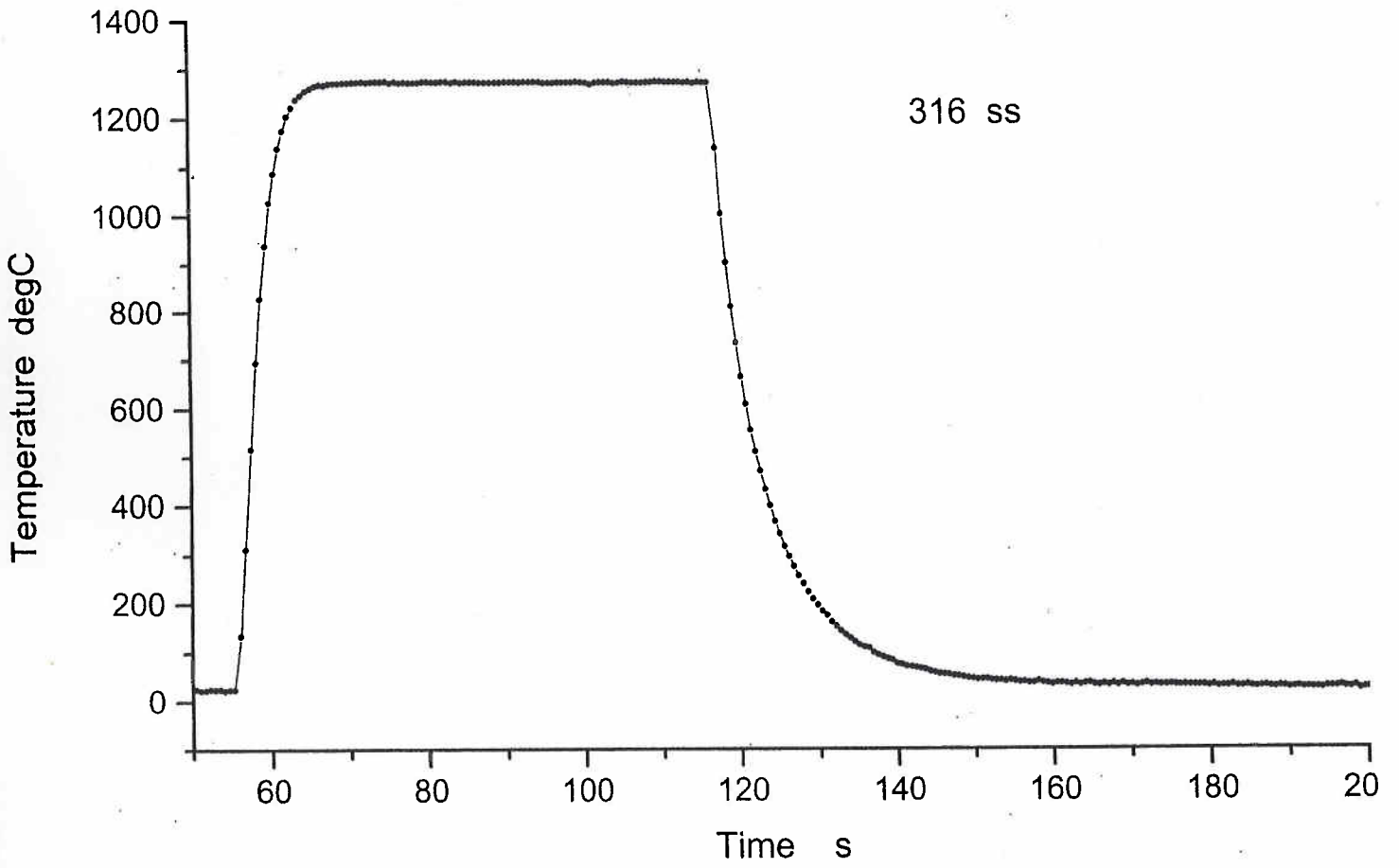


Fig 16 Heating rate to 1300 °C for 316 stainless testpiece.

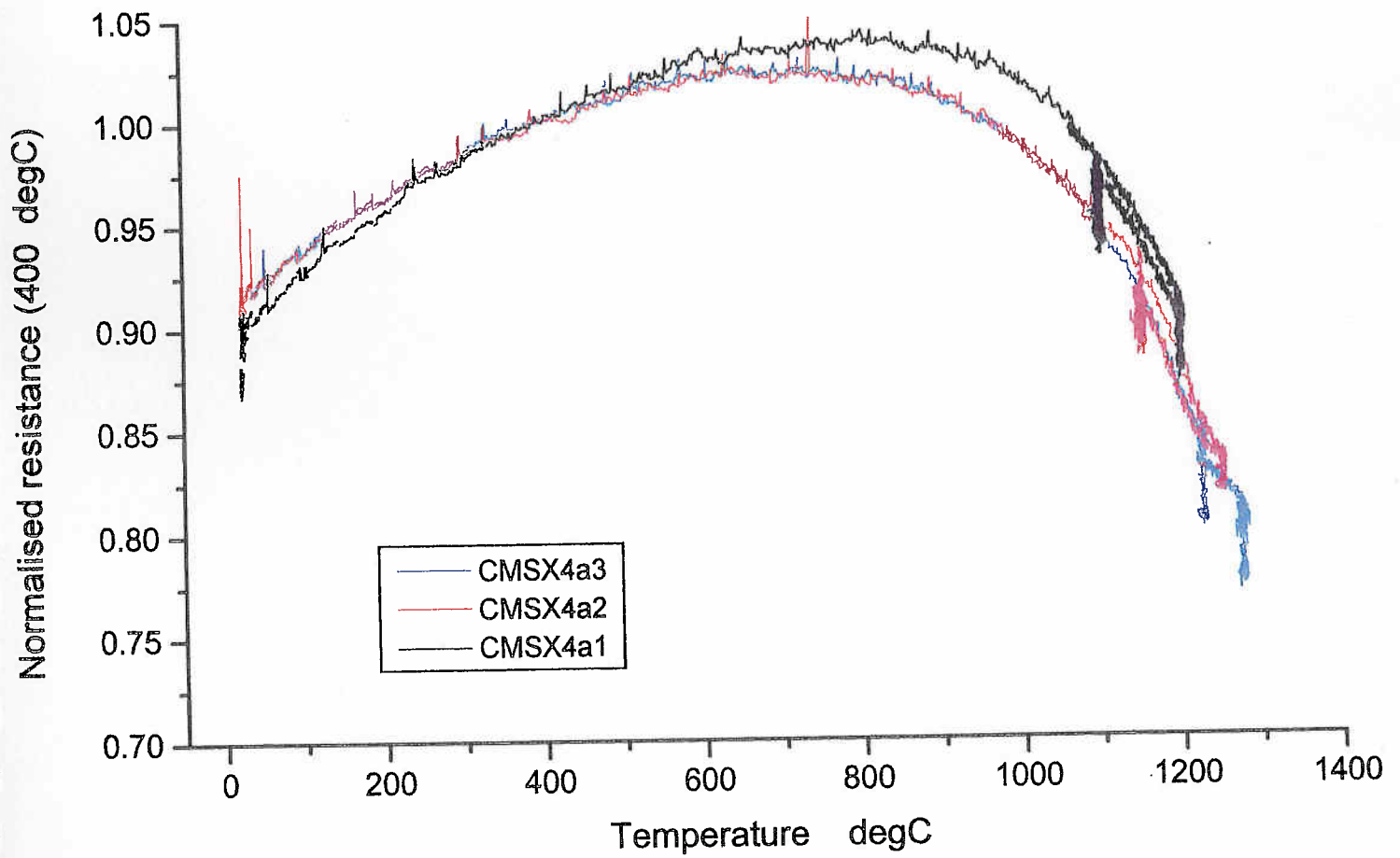


Fig 17 Normalised resistance/temperature plot for tests on CMSX4a.

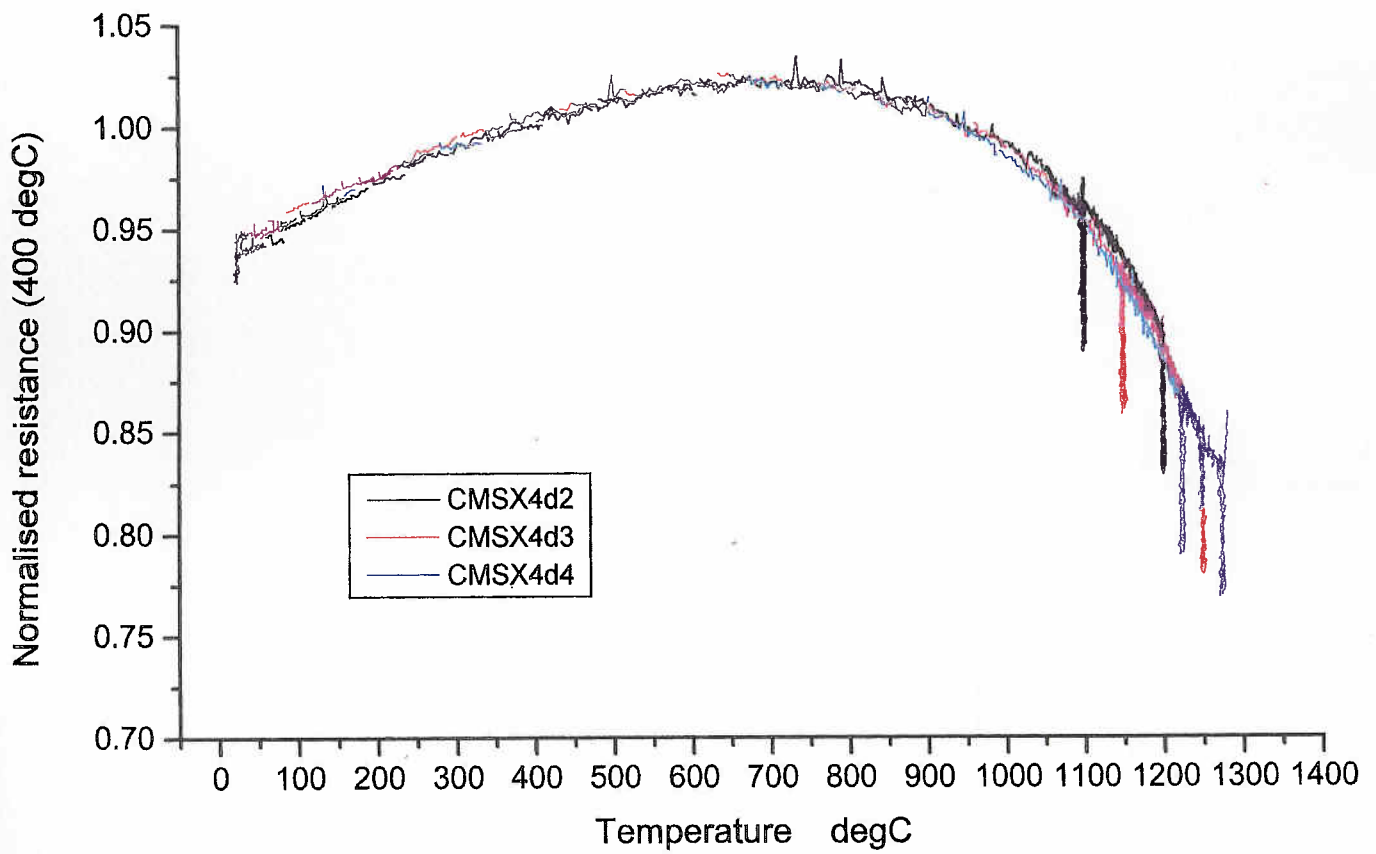


Fig 18 Normalised resistance/temperature plot for tests on CMSX4d.

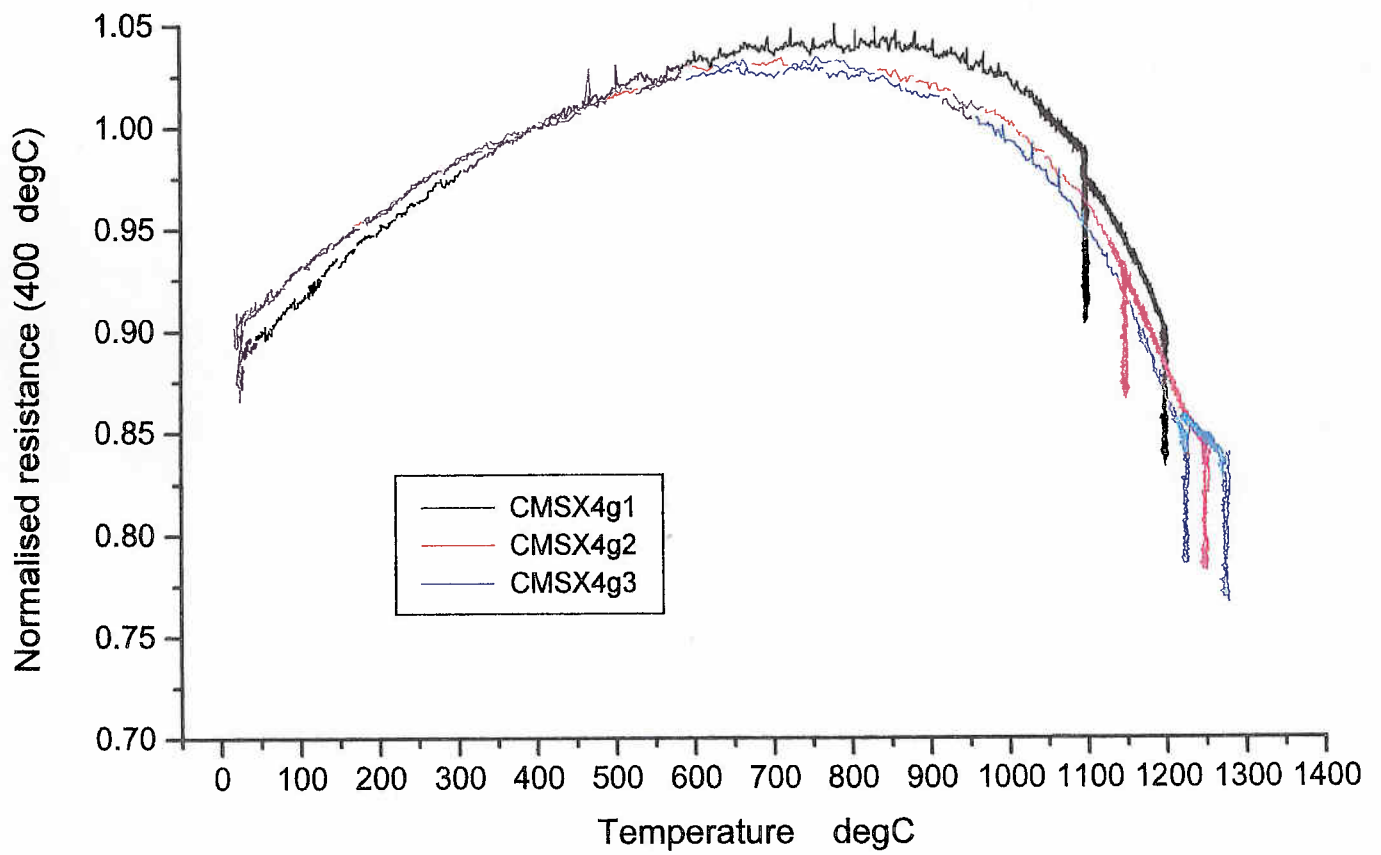


Fig 19 Normalised resistance/temperature plot for tests on CMSX4g.

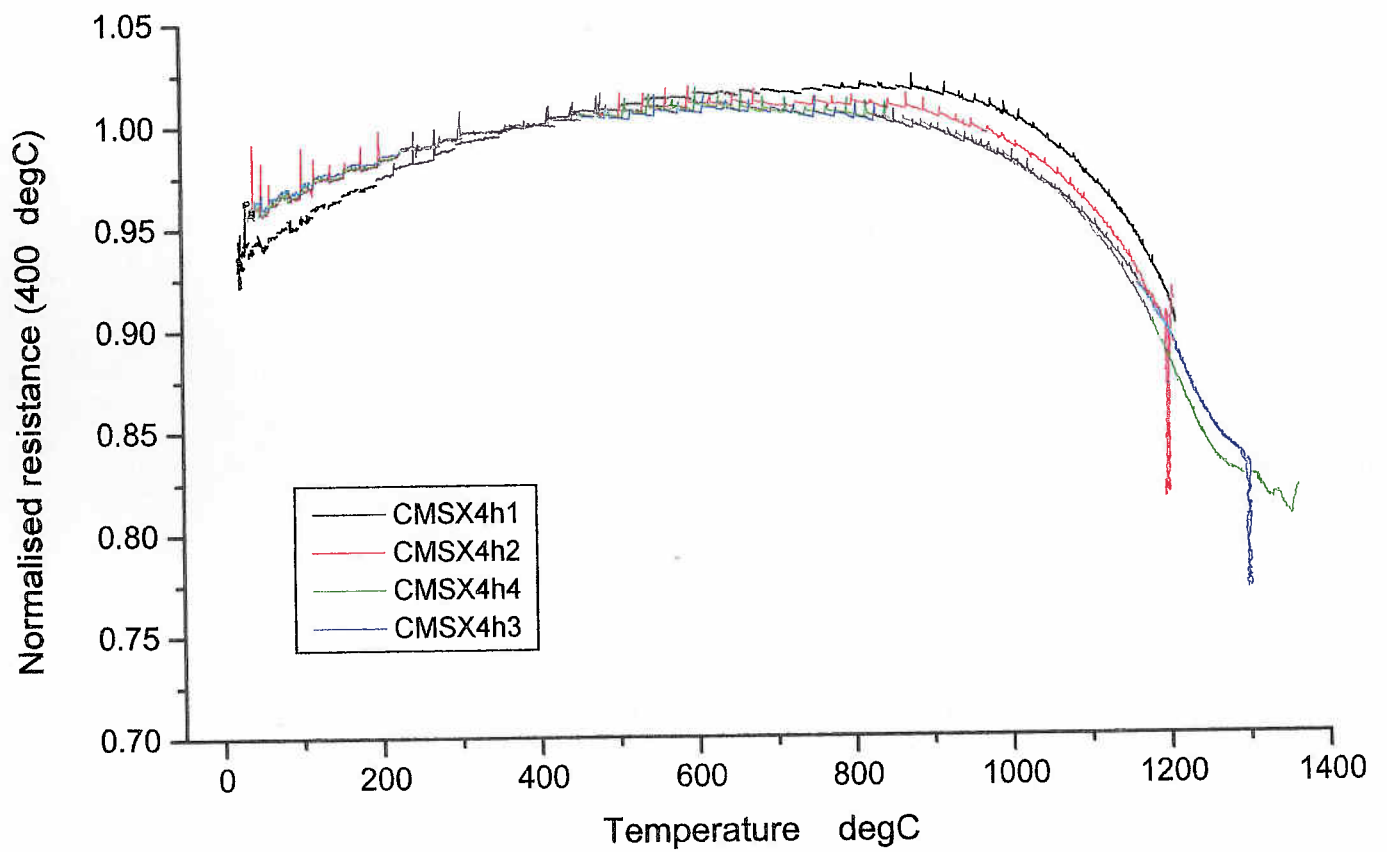


Fig 20 Normalised resistance/temperature plot for tests on CMSX4h.

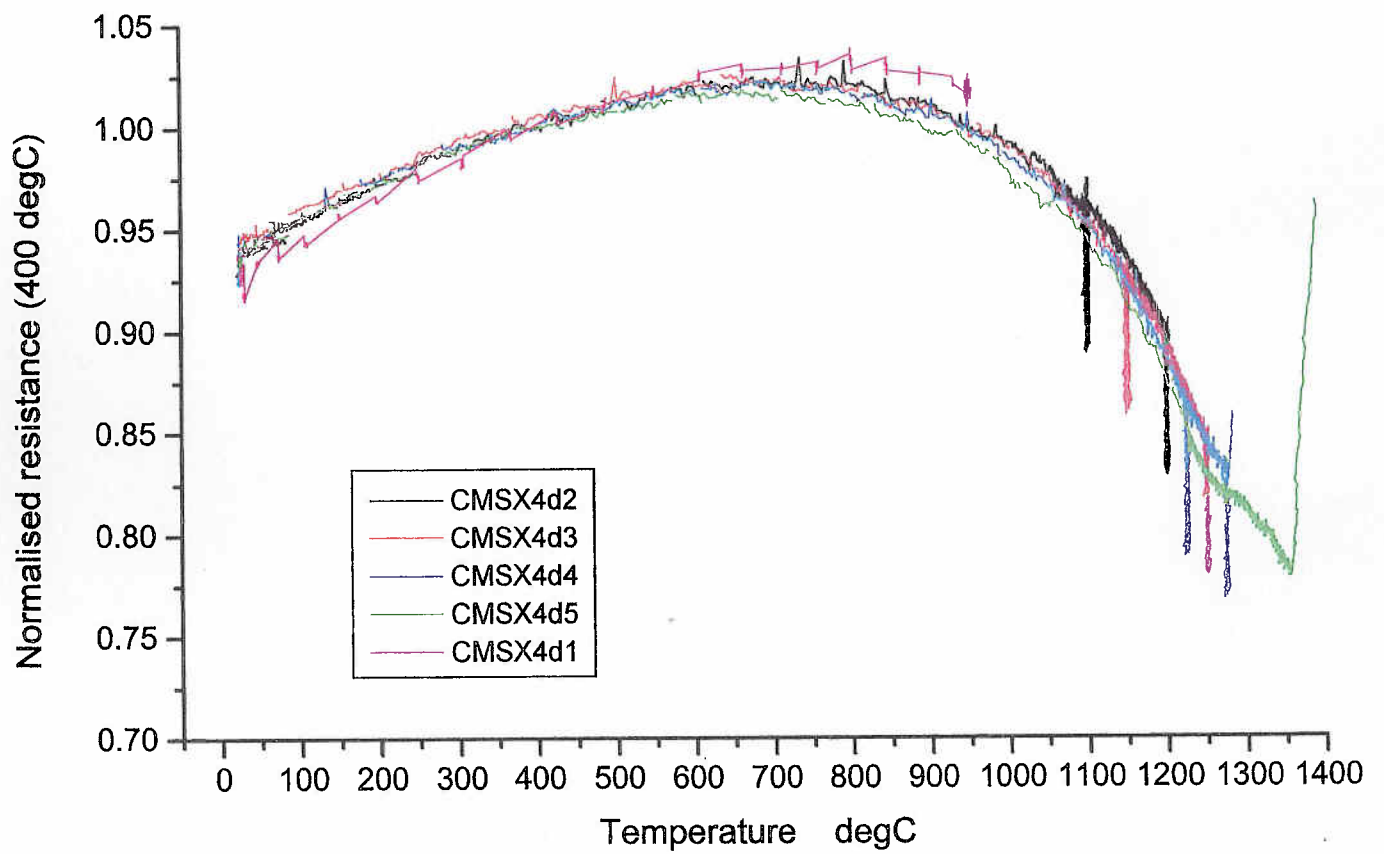


Fig 21 Normalised resistance/temperature plot for tests on CMSX4d, showing heating cycle to solidus.

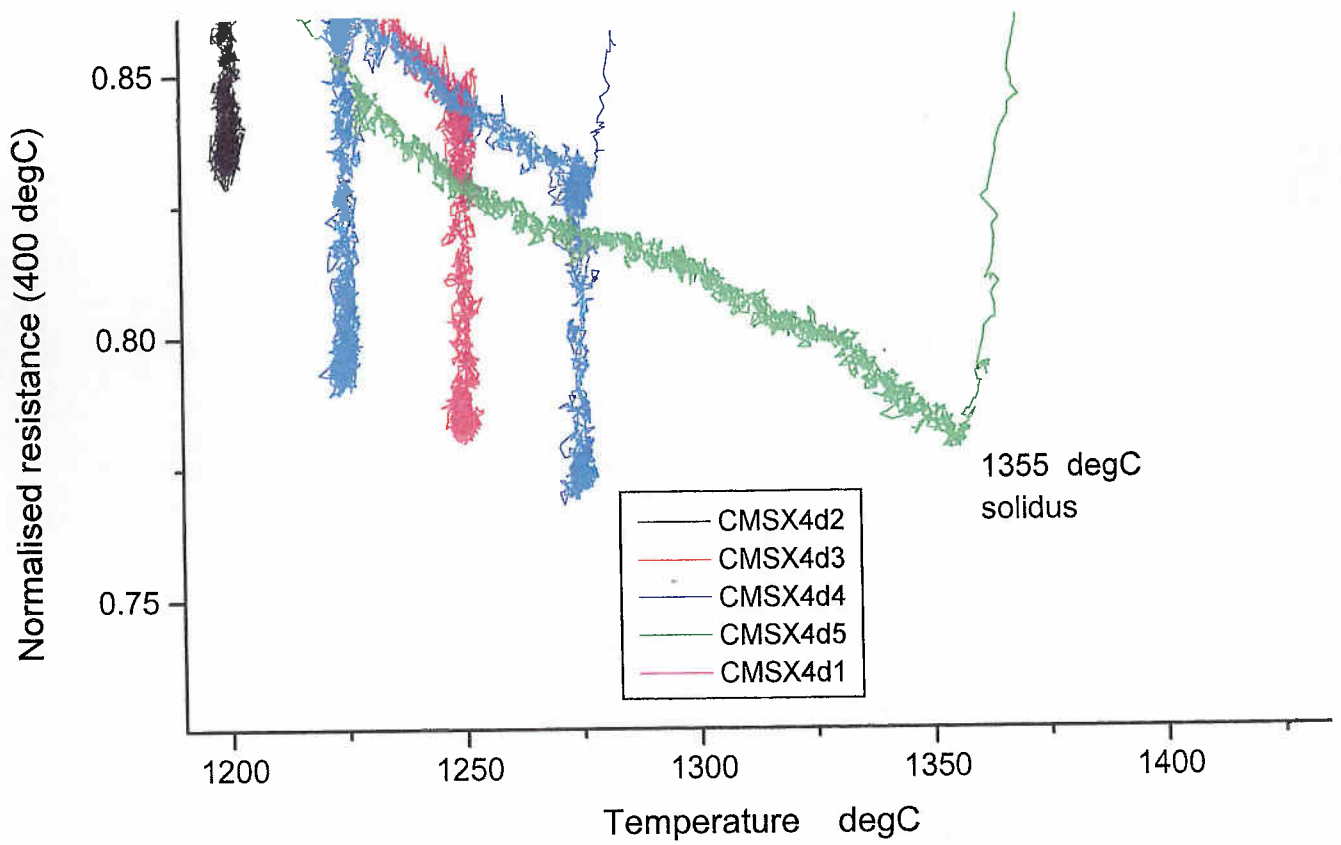


Fig 22 Expanded plot of Fig 21 on CMSX4d.

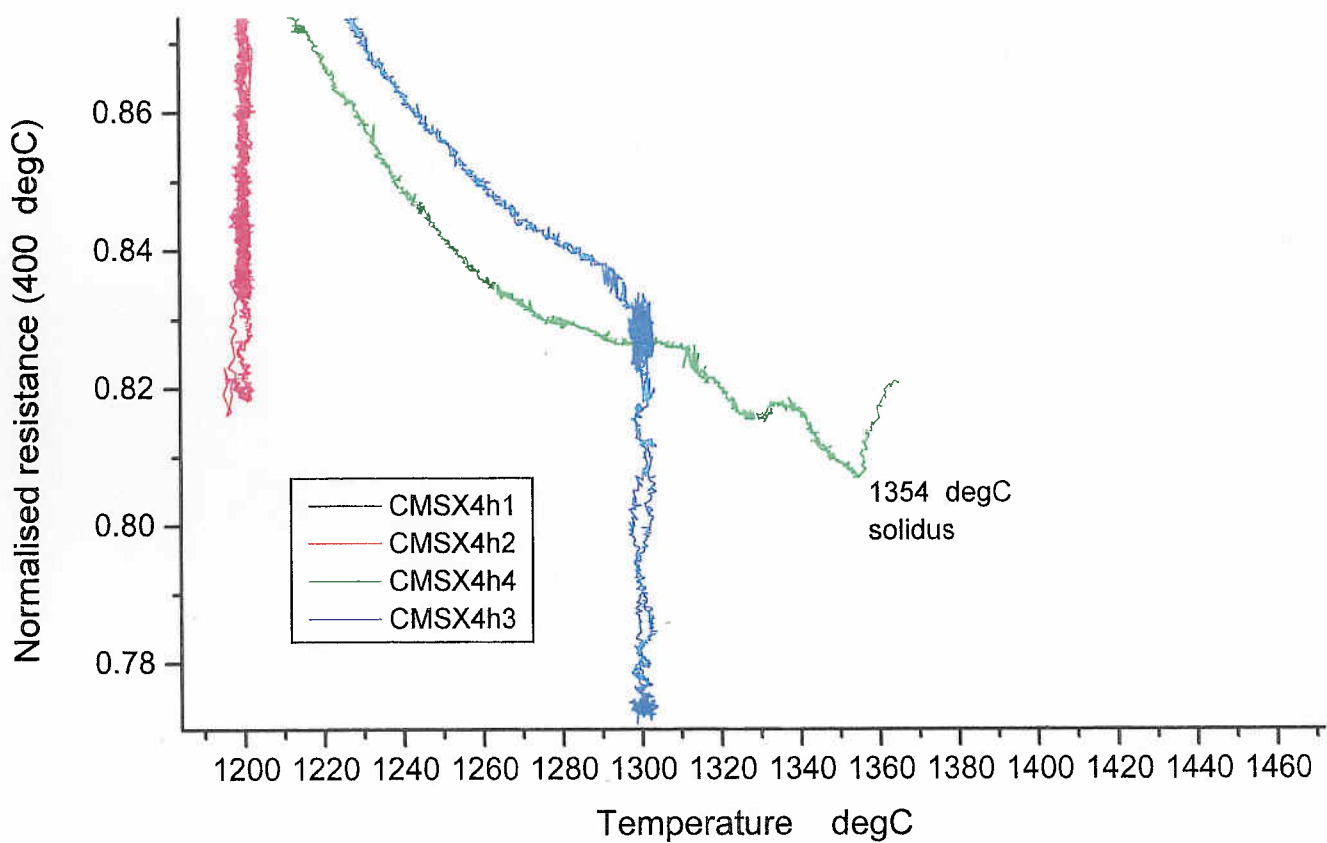


Fig 23 Expanded plot of Fig 20 on CMSX4h.

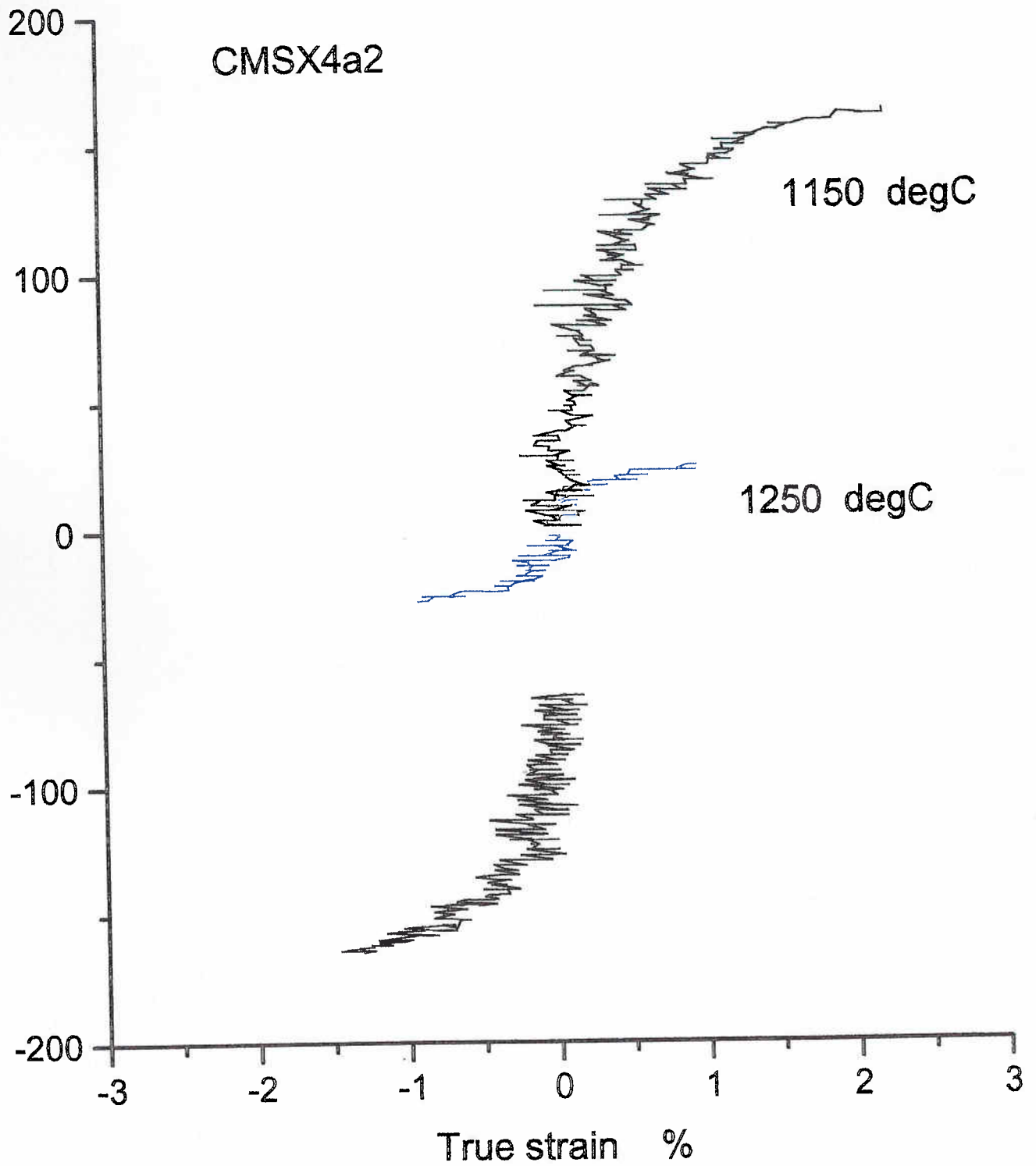


Fig 24 Stress/strain plot in tension and compression at 1150 °C and 1250 °C for CMSX4a2 (rod VFV4).

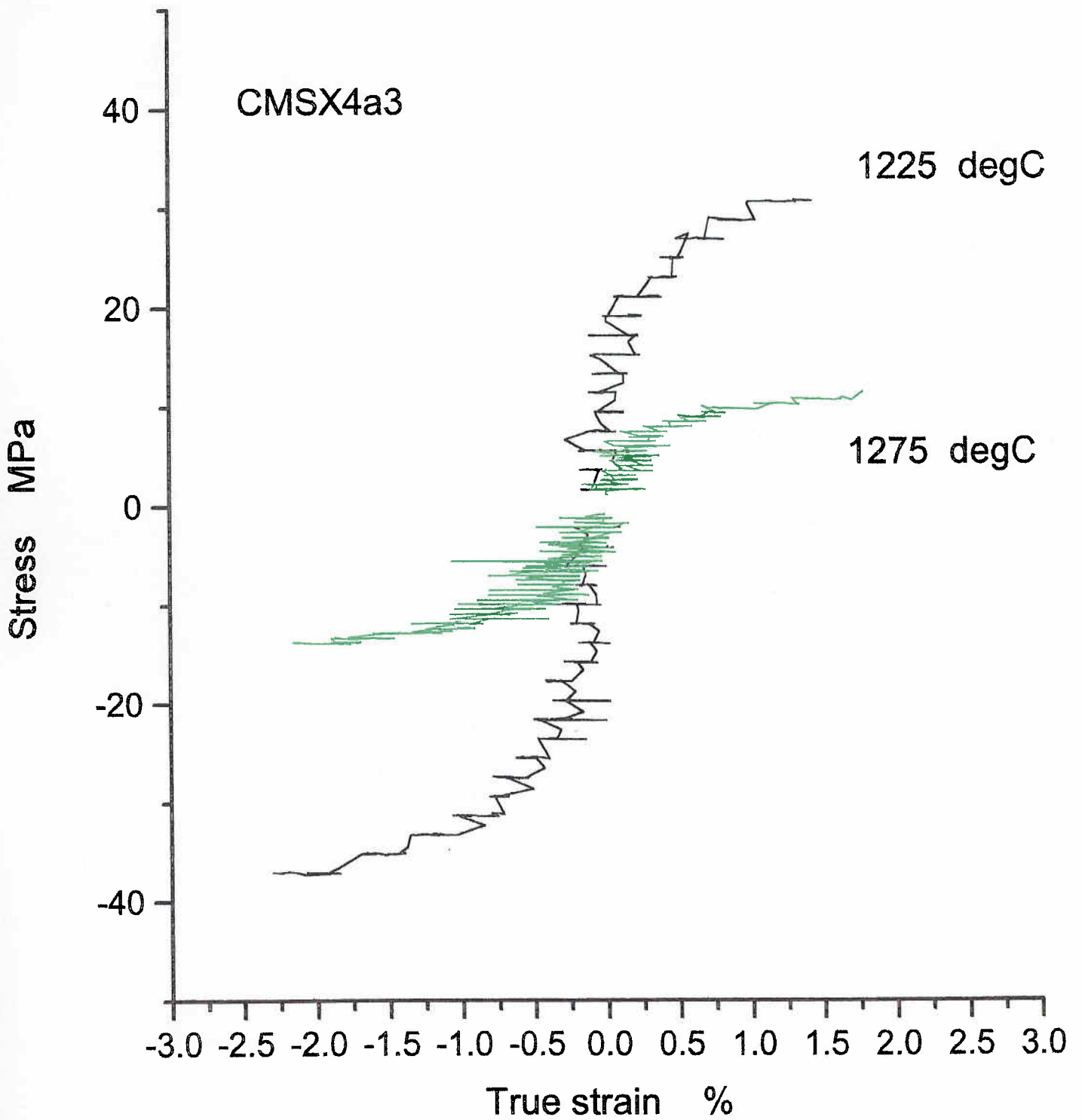


Fig 25 Stress/strain plot in tension and compression at 1225 °C and 1275 °C for CMSX4a3 (rod VFV4).

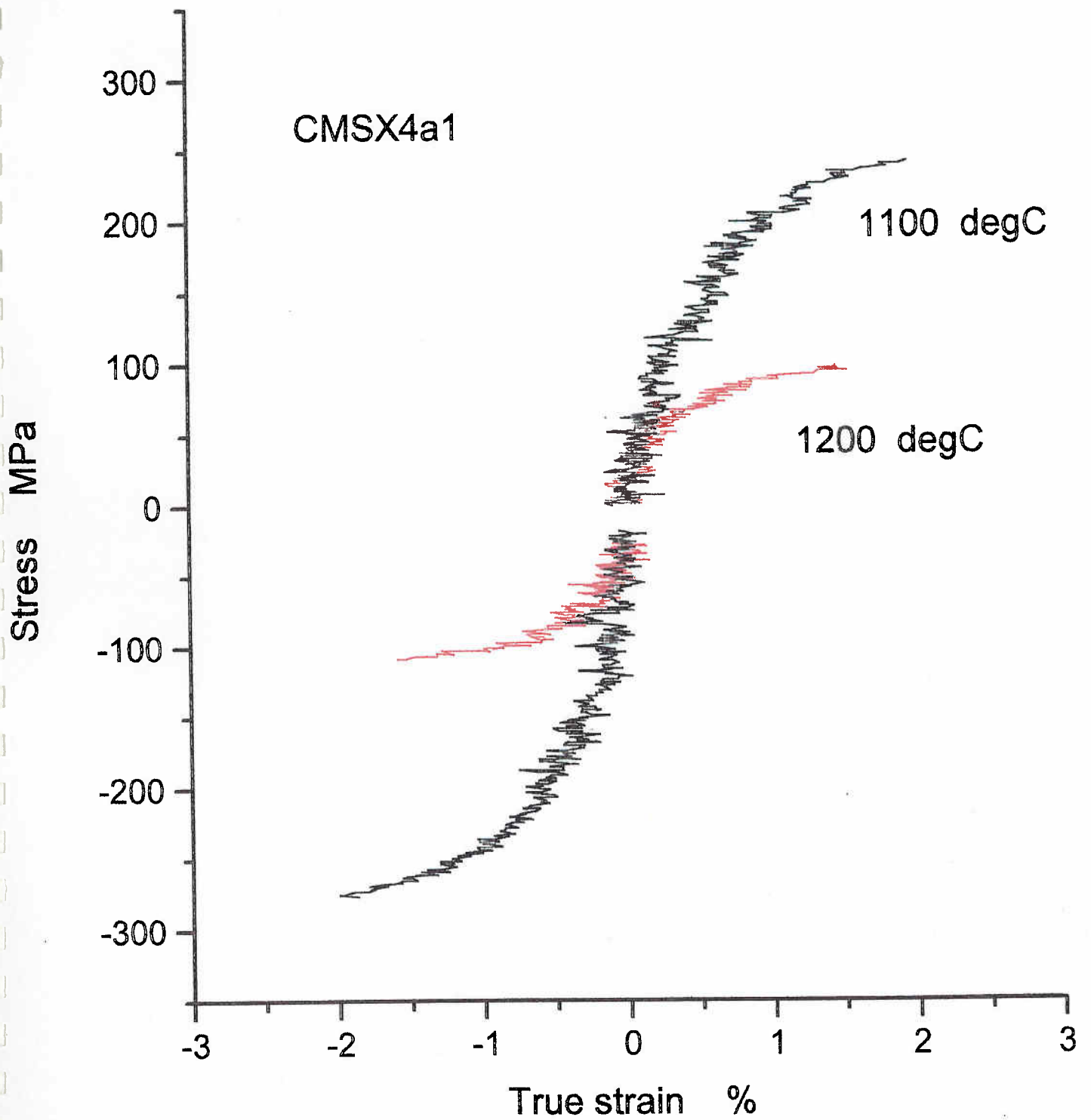


Fig 26 Stress/strain plot in tension and compression at 1100 °C and 1200 °C for CMSX4a1 (rod VFV4).

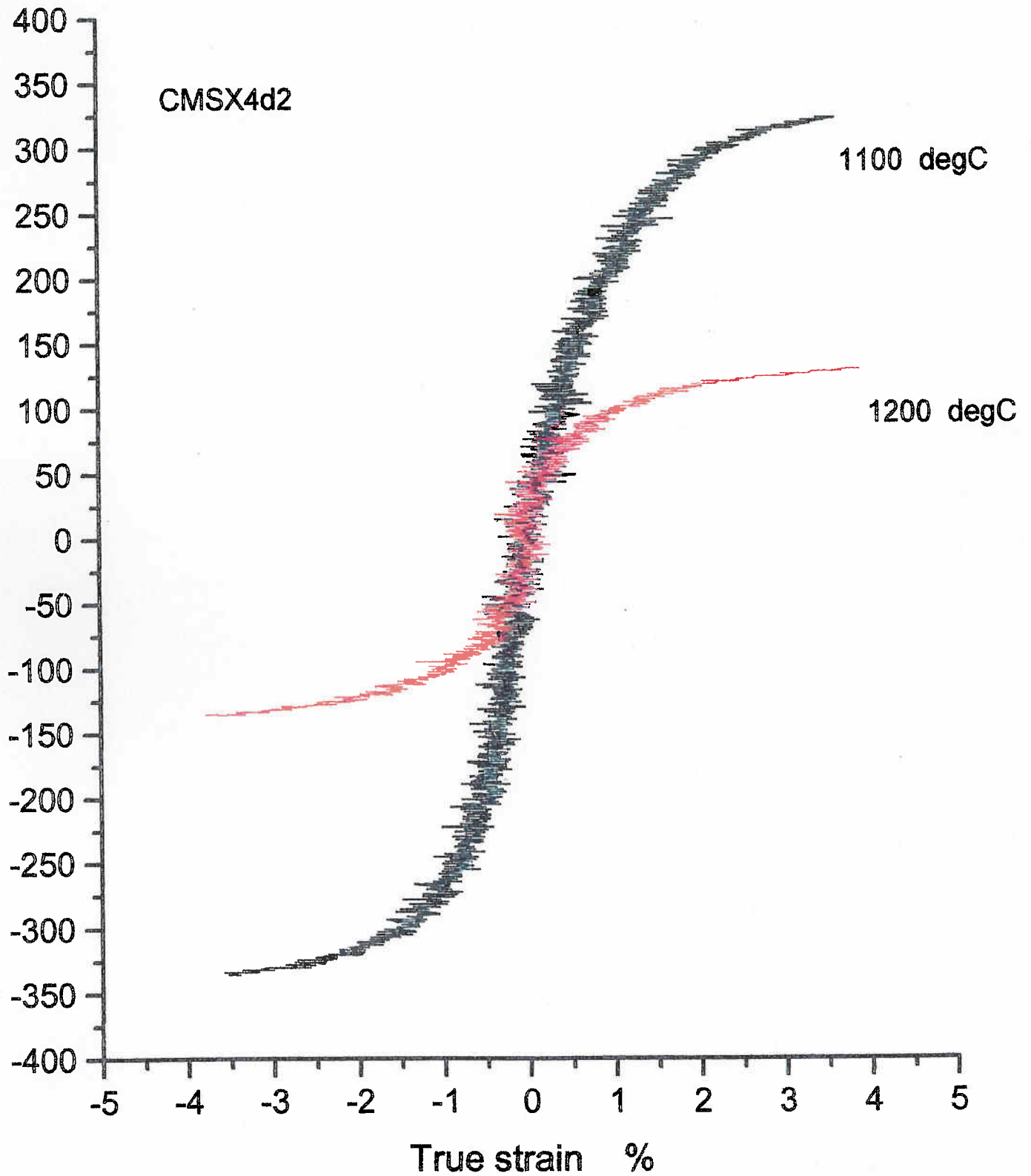


Fig 27 Stress/strain plot in tension and compression at 1100 °C and 1200 °C for CMSX4d2 (rod VFV7).

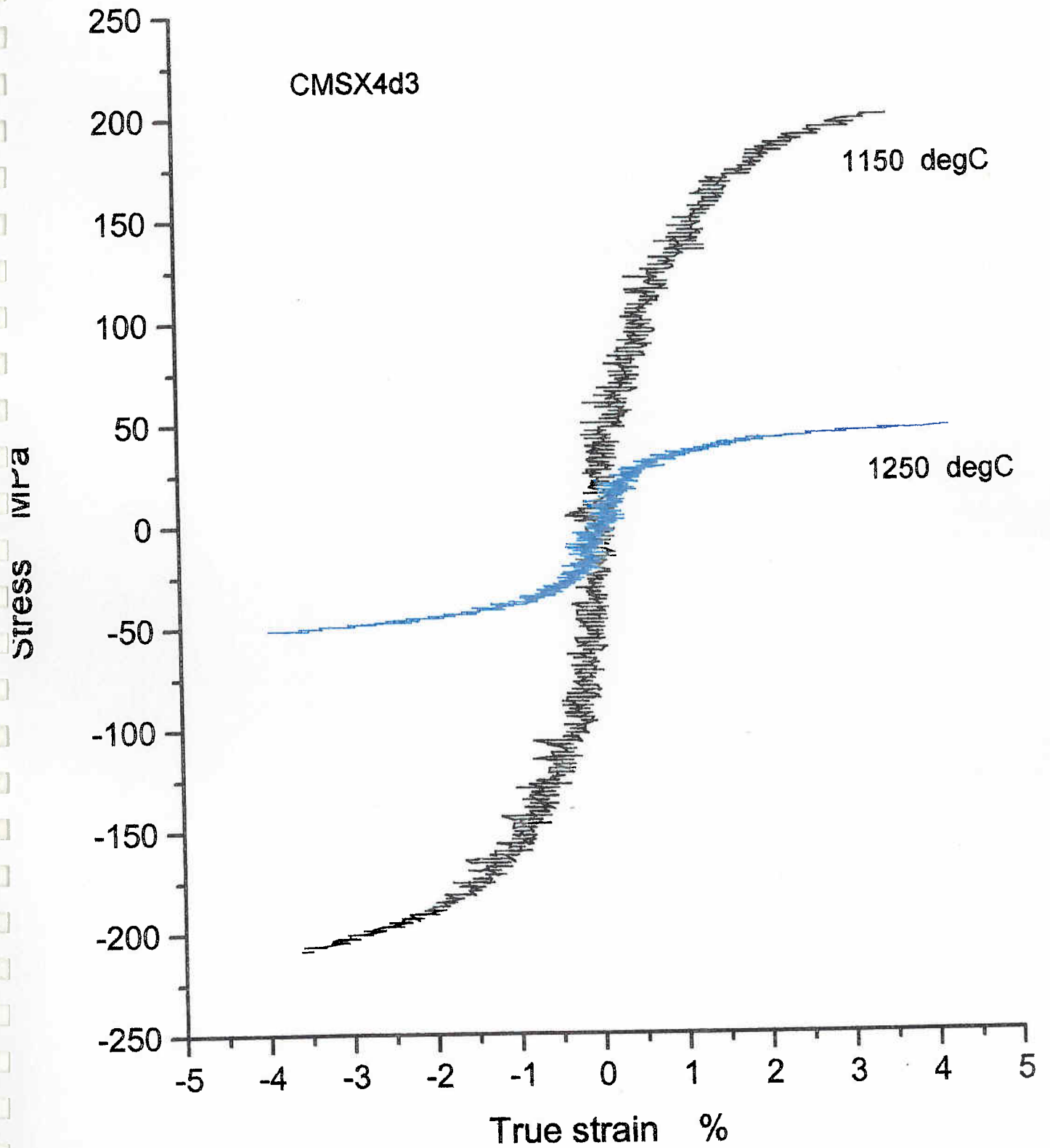


Fig 28 Stress/strain plot in tension and compression at 1150 °C and 1250 °C for CMSX4d3 (rod VFW7).

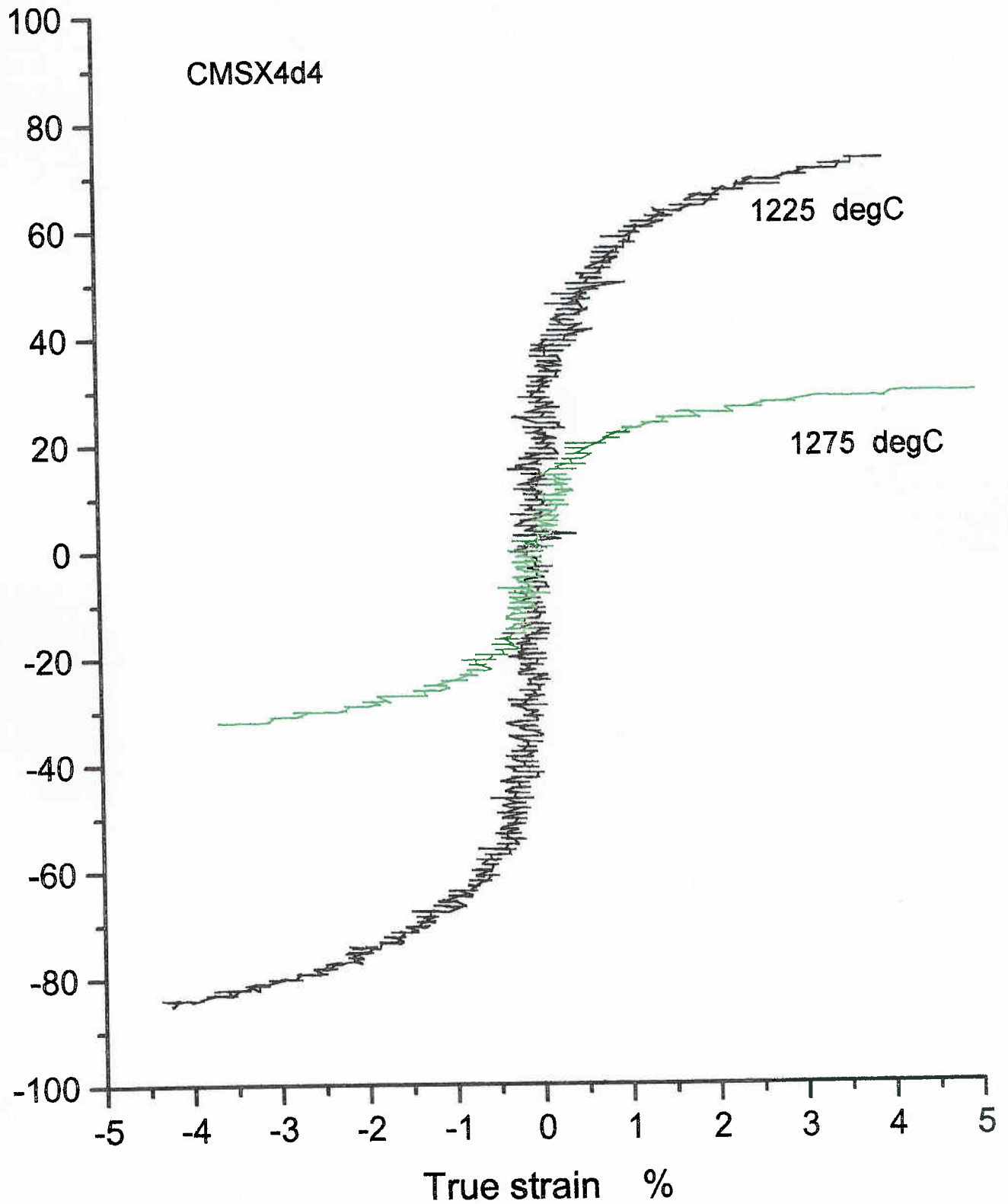


Fig 29 Stress/strain plot in tension and compression at 1225 °C and 1275 °C for CMSX4d4 (rod VFV7).

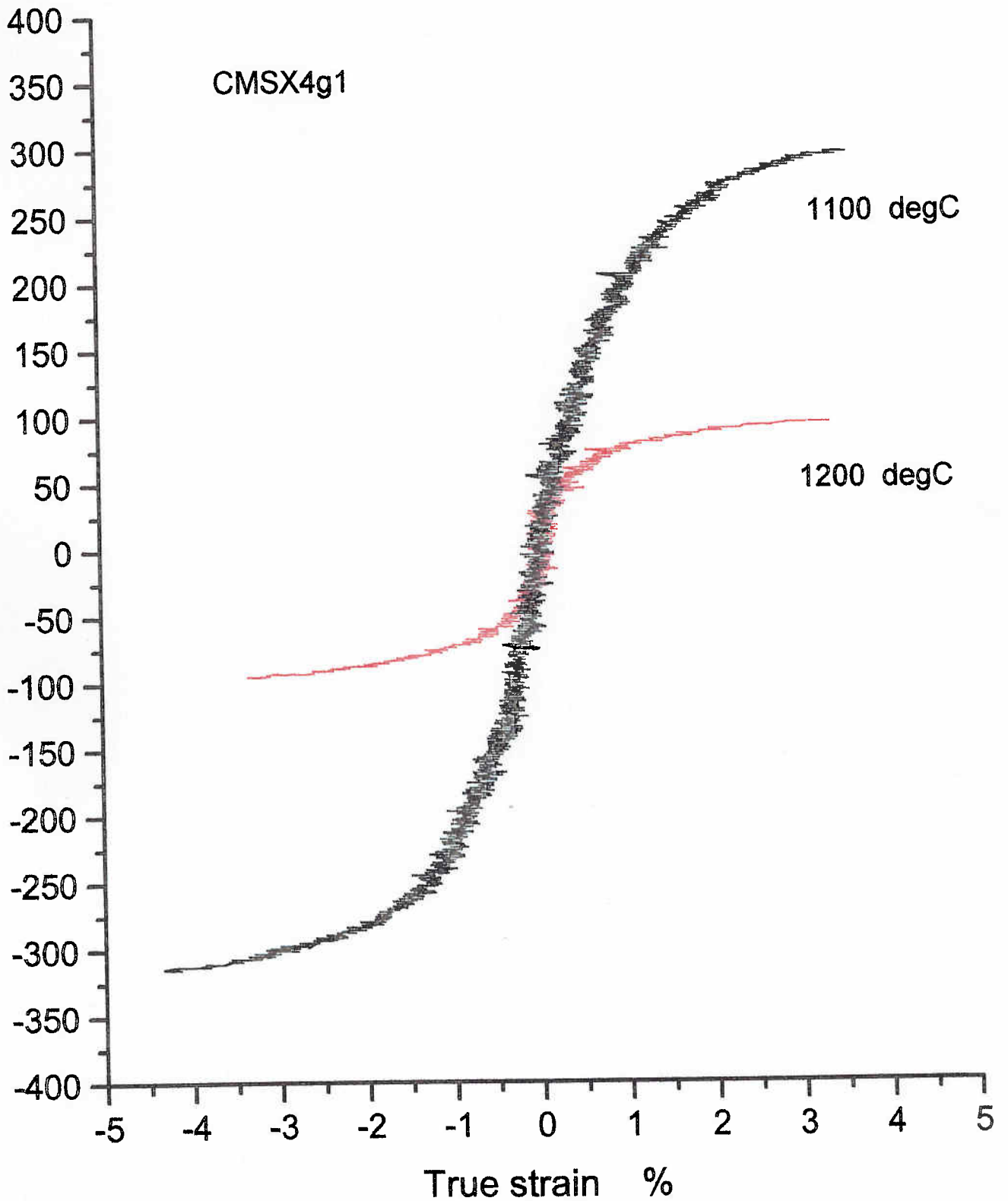


Fig 30 Stress/strain plot in tension and compression at 1100 °C and 1200 °C for CMSX4g1 (rod VFV1).

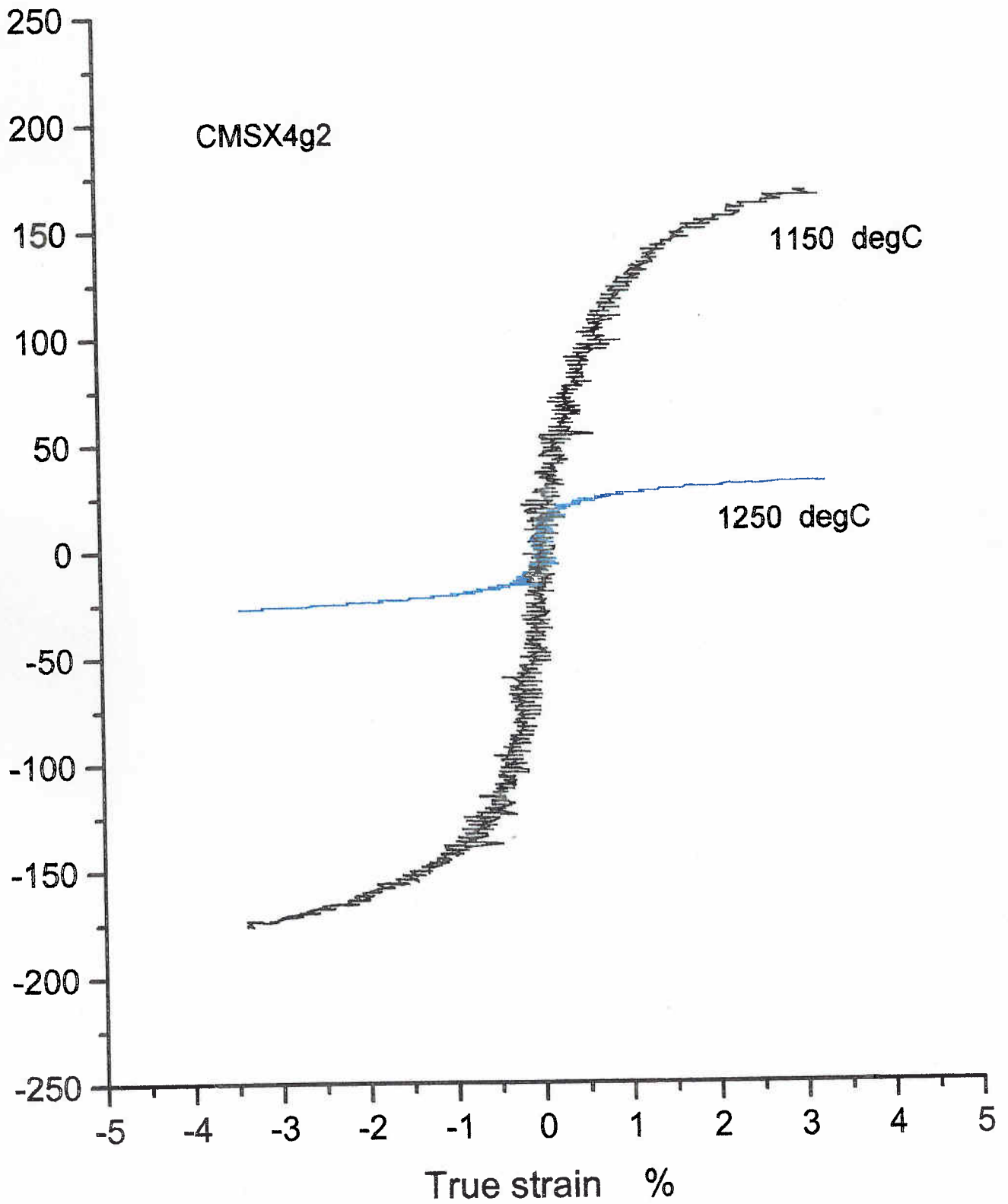


Fig 31 Stress/strain plot in tension and compression at 1150 °C and 1250 °C for CMSX4g2 (rod VFV1).

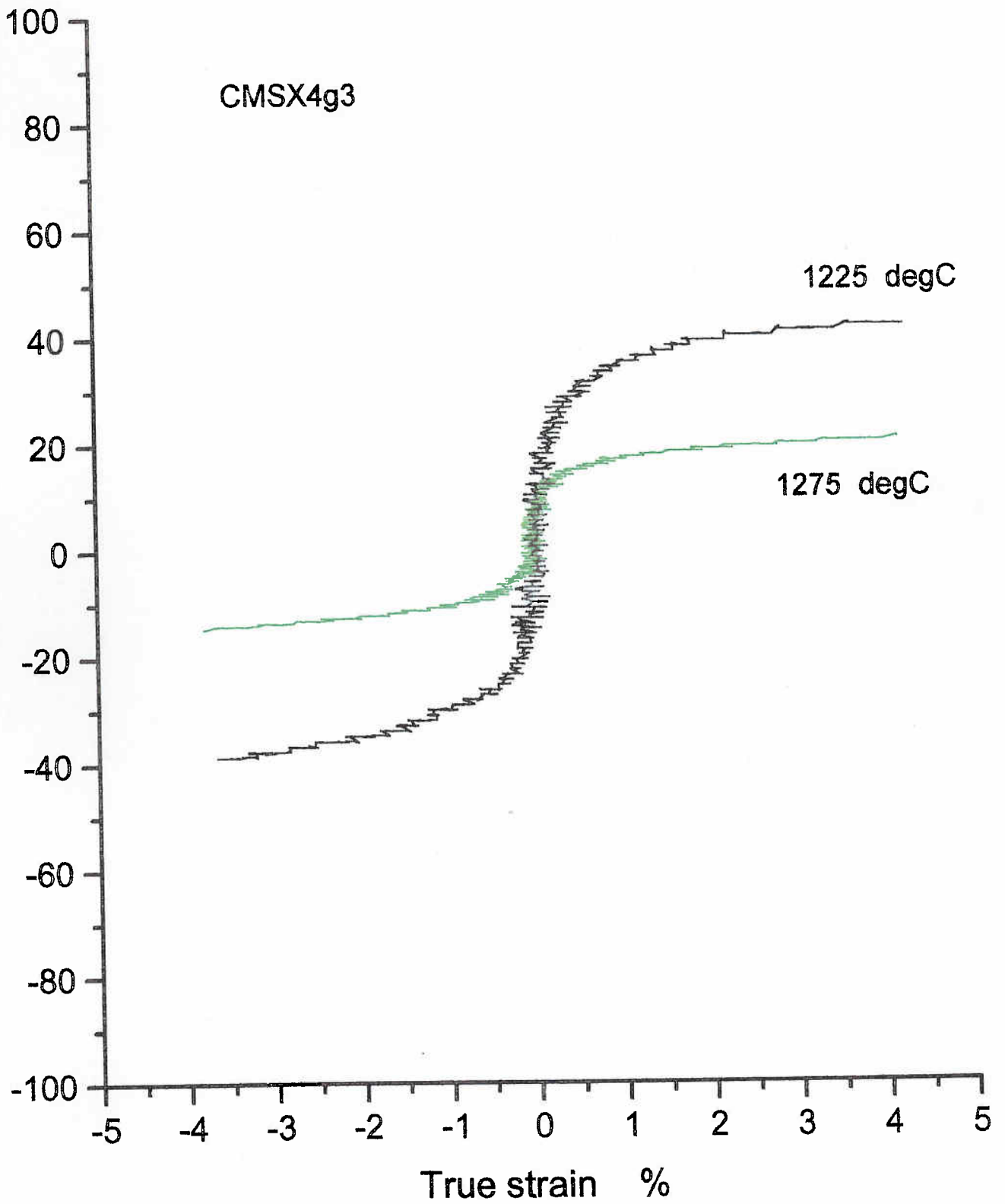


Fig 32 Stress/strain plot in tension and compression at 1225 °C and 1275 °C for CMSX4g3 (rod VFV1).

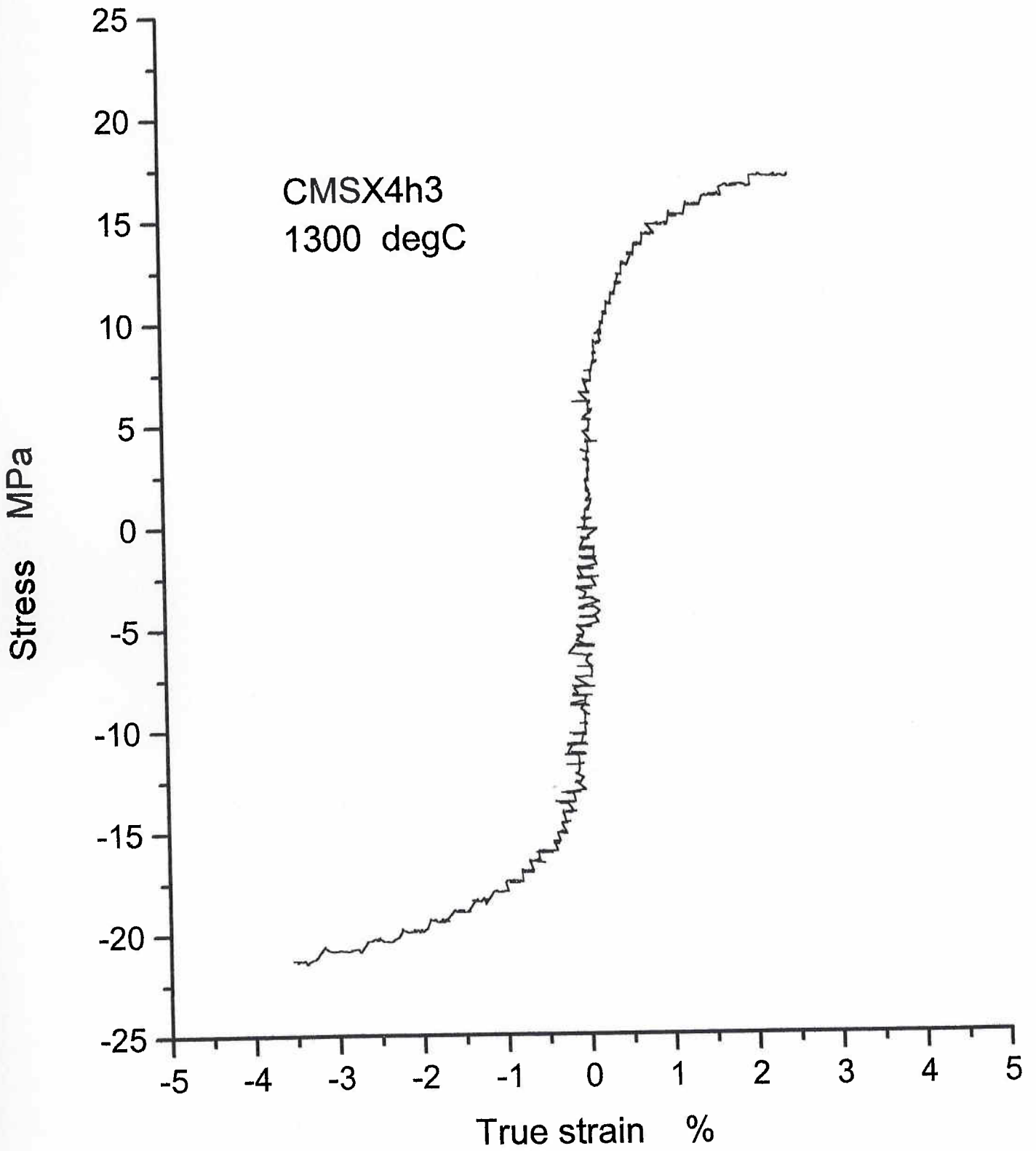


Fig 33 Stress/strain plot in tension and compression at 1300 °C for CMSX4h3 (rod VFV1).

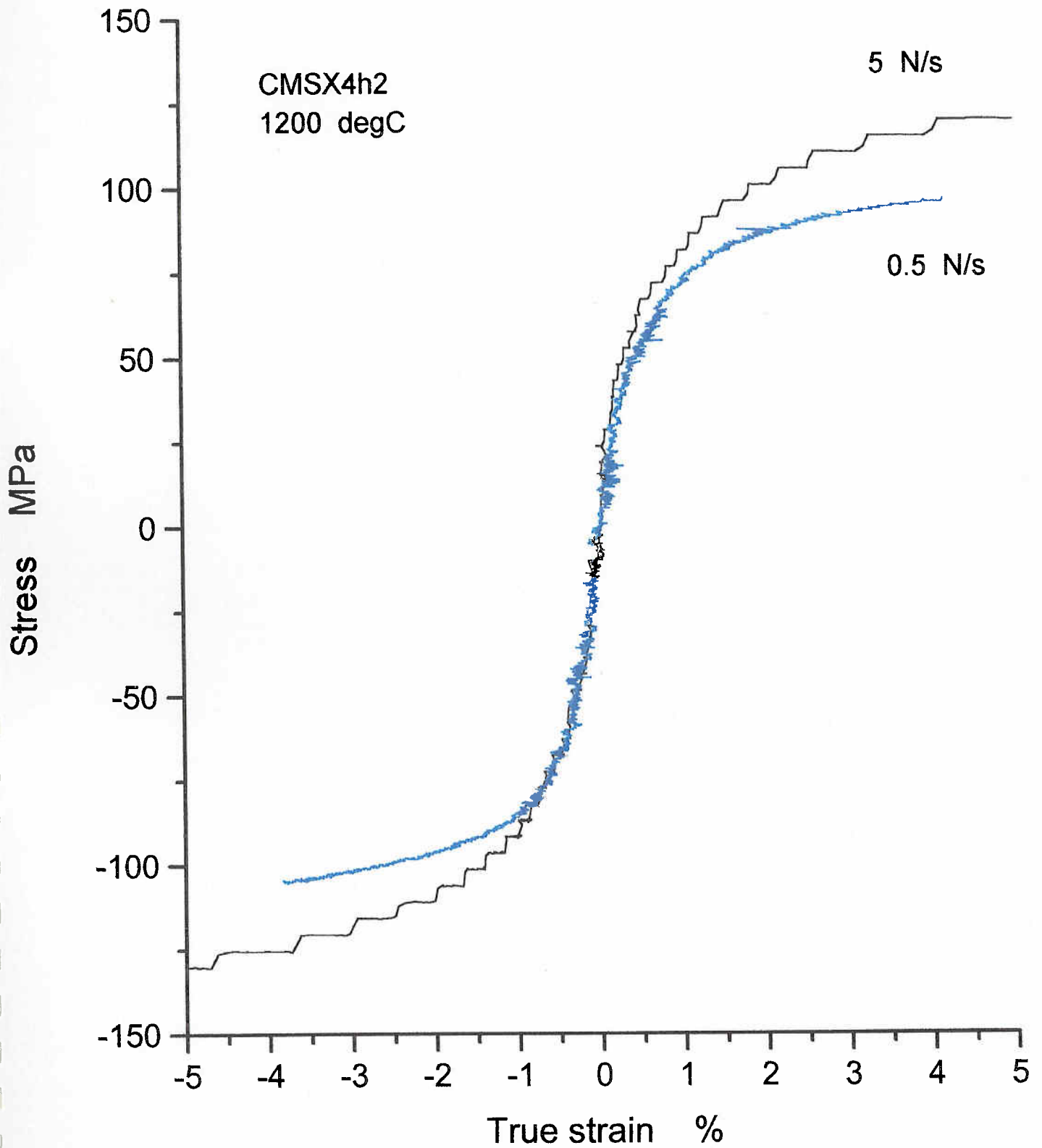


Fig 34 Stress/strain plots at different loading rates at 1200 °C for CMSX4h2 (rod VFV1).

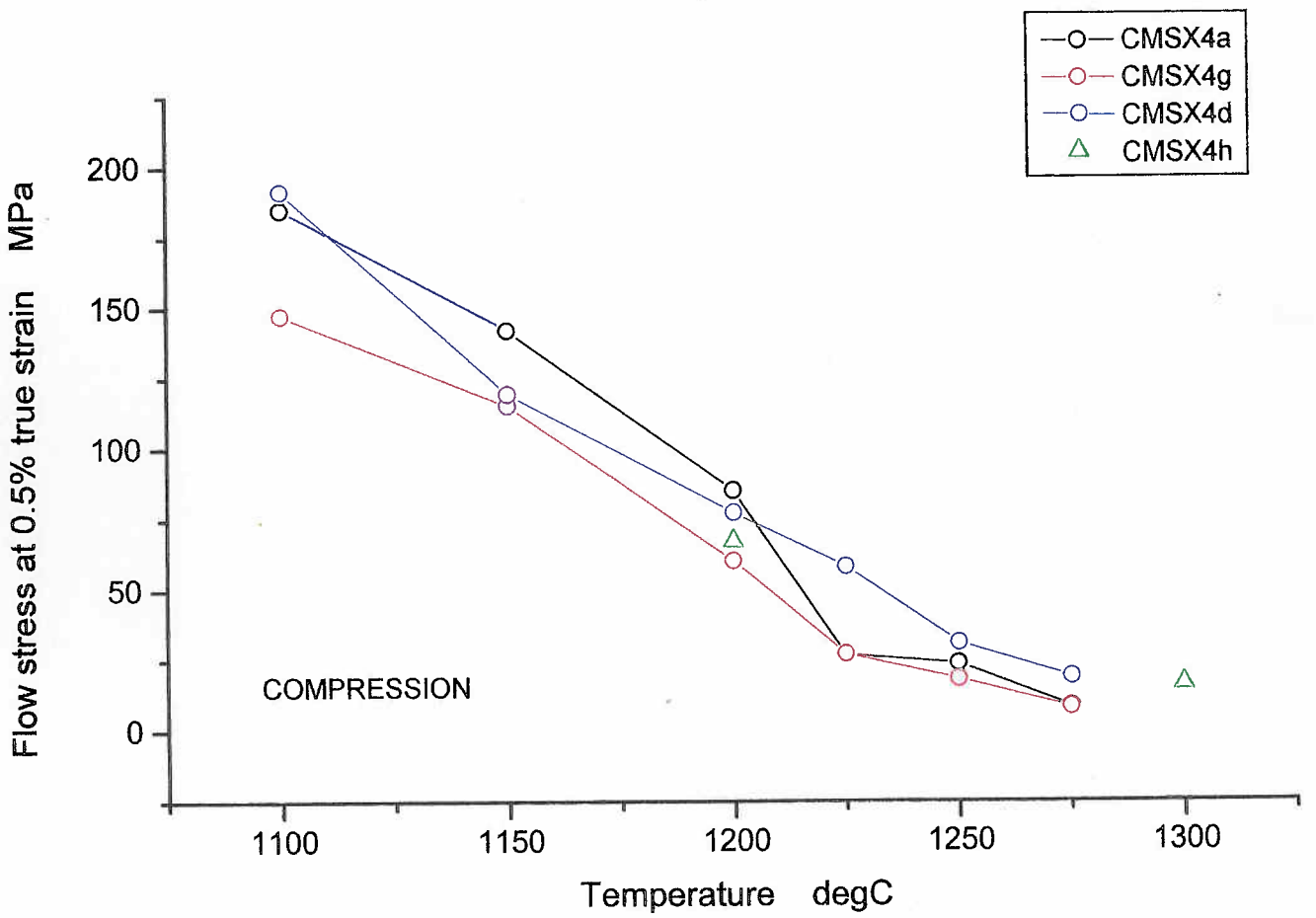


Fig 35 Flow stress at 0.5% strain in compression on CMSX4.

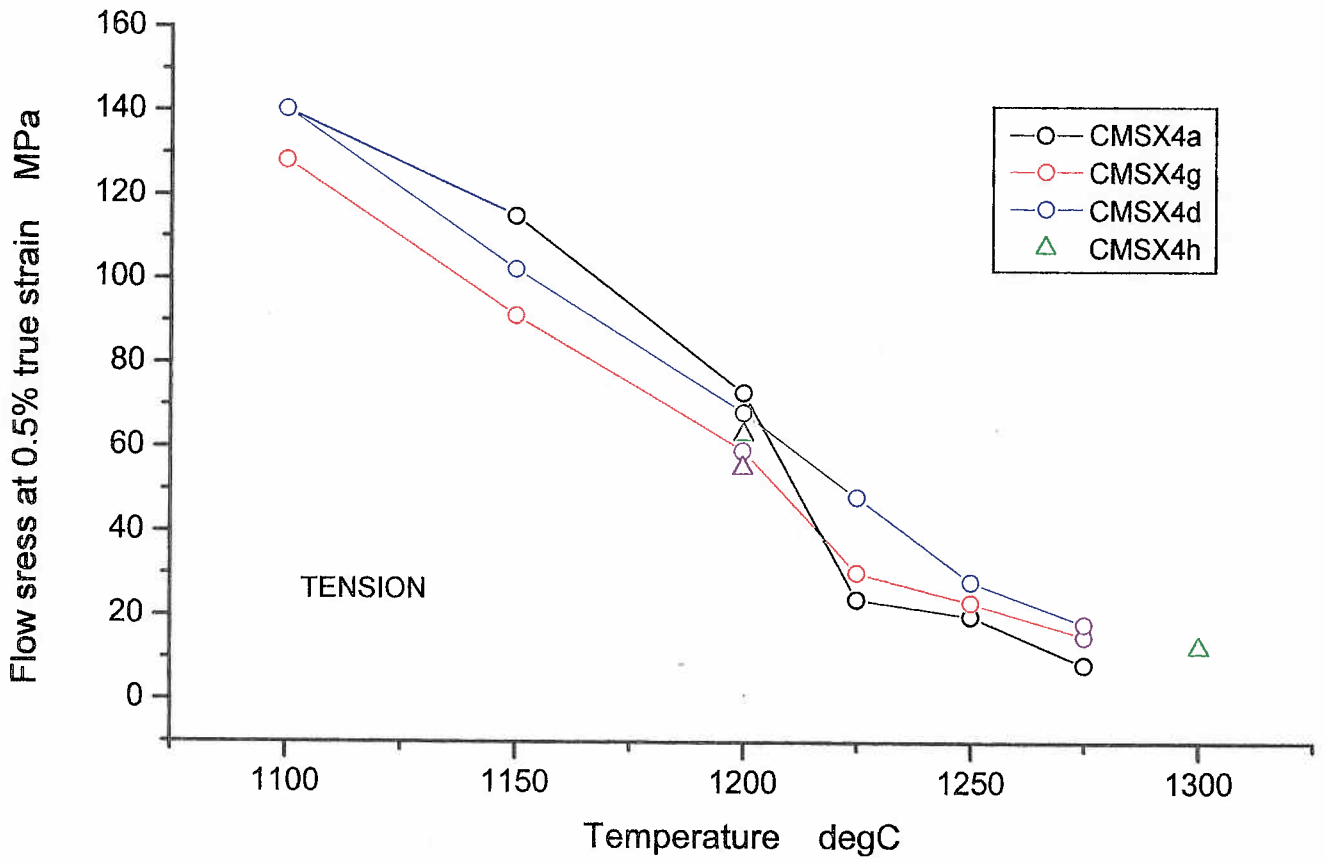


Fig 36 Flow stress at 0.5% strain in tension on CMSX4.

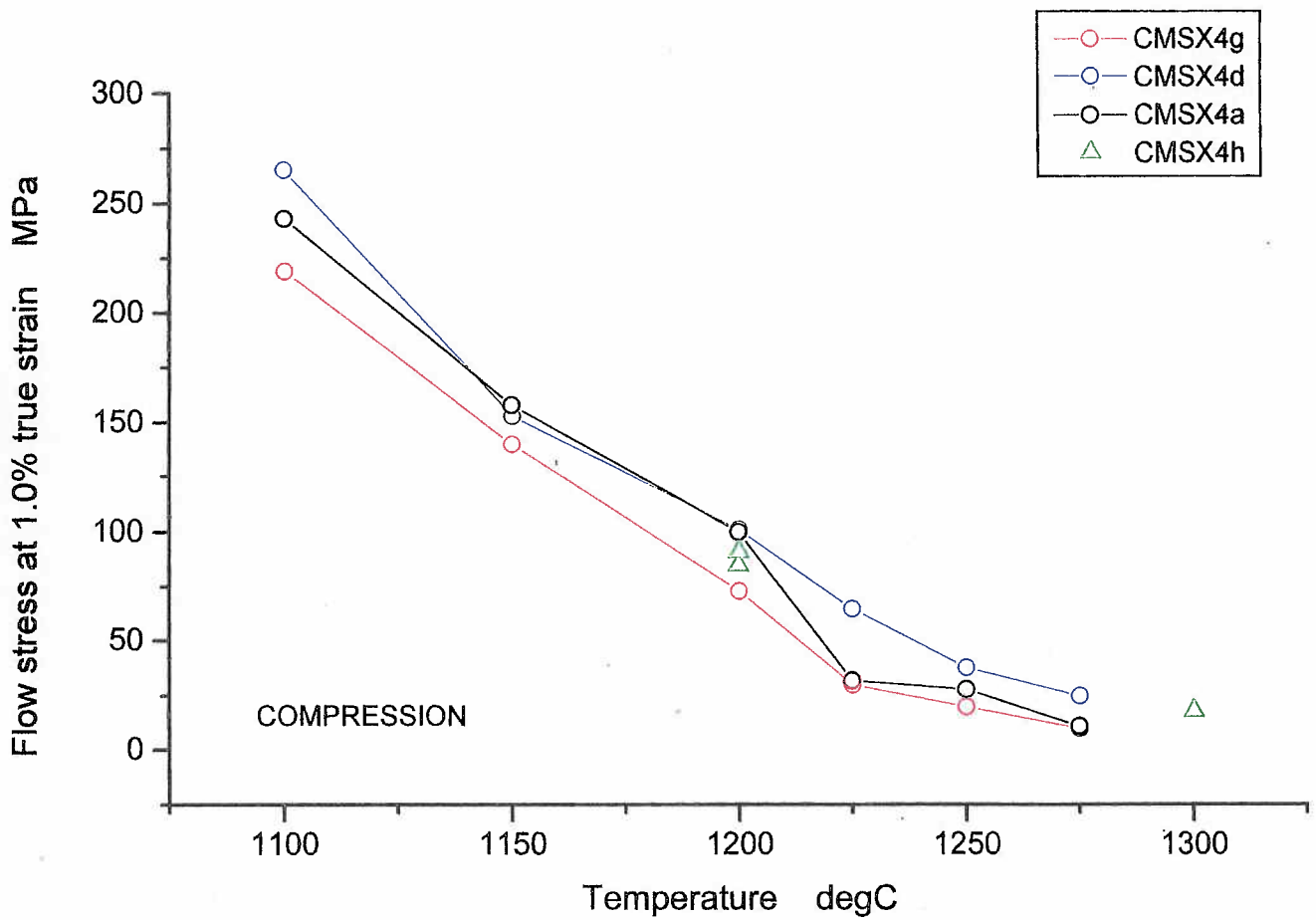


Fig 37 Flow stress at 1.0% strain in compression on CMSX4.

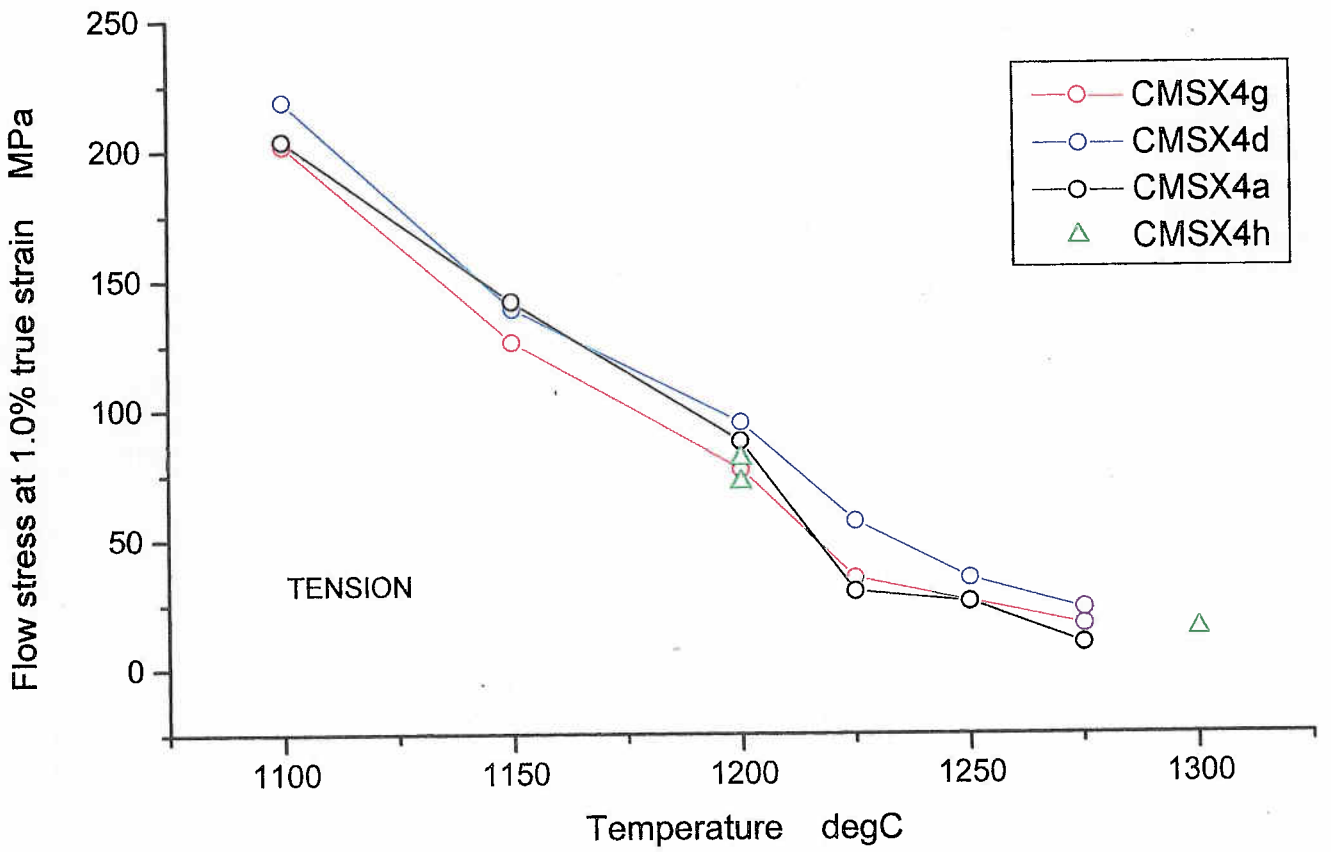


Fig 38 Flow stress at 1.0% strain in tension on CMSX4.

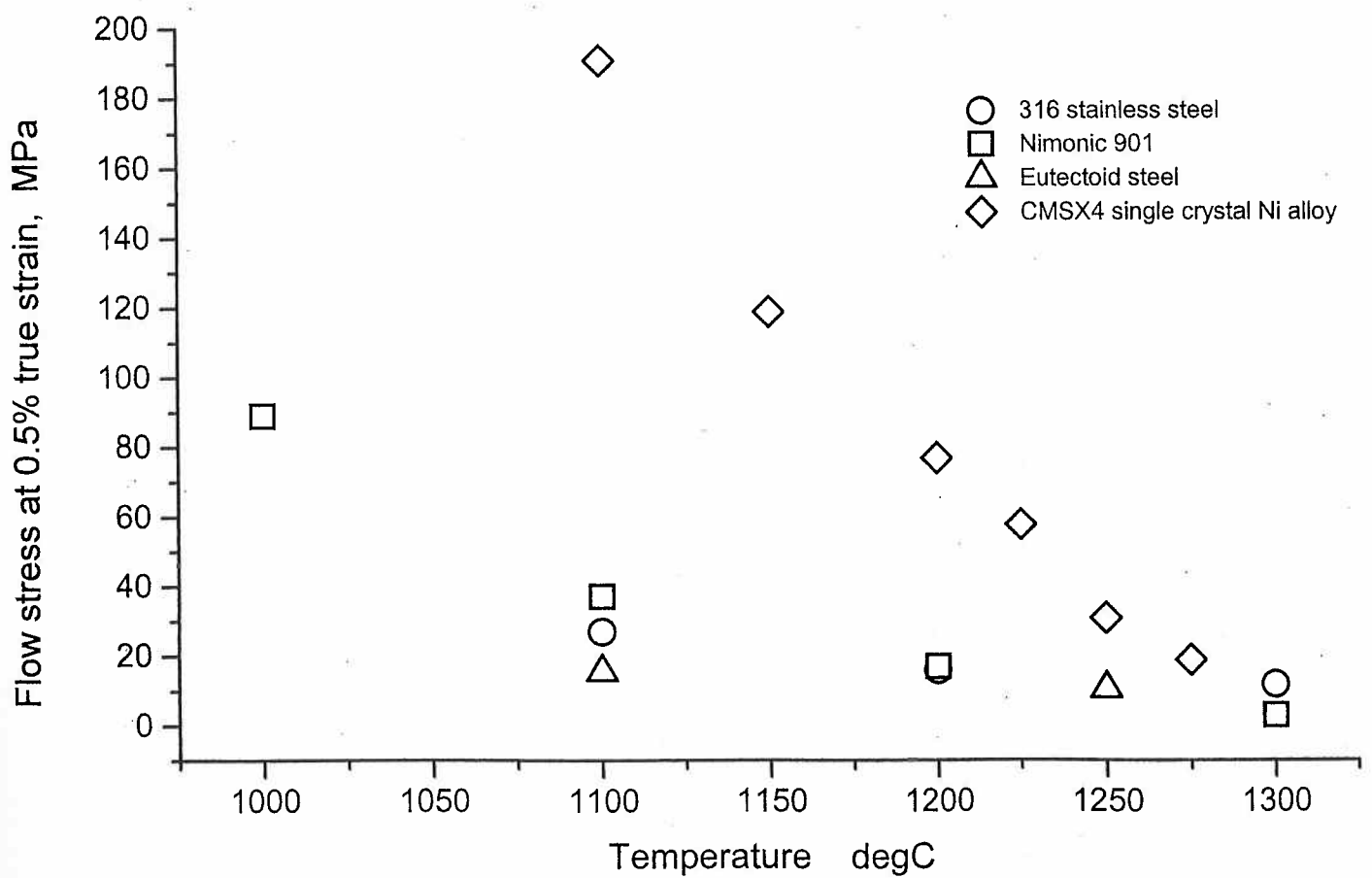


Fig 39 Flow stress at 0.5% strain for tests on Nimonic 901, 316 stainless steel, CMSX4 single crystal Ni alloy and Eutectoid steel.

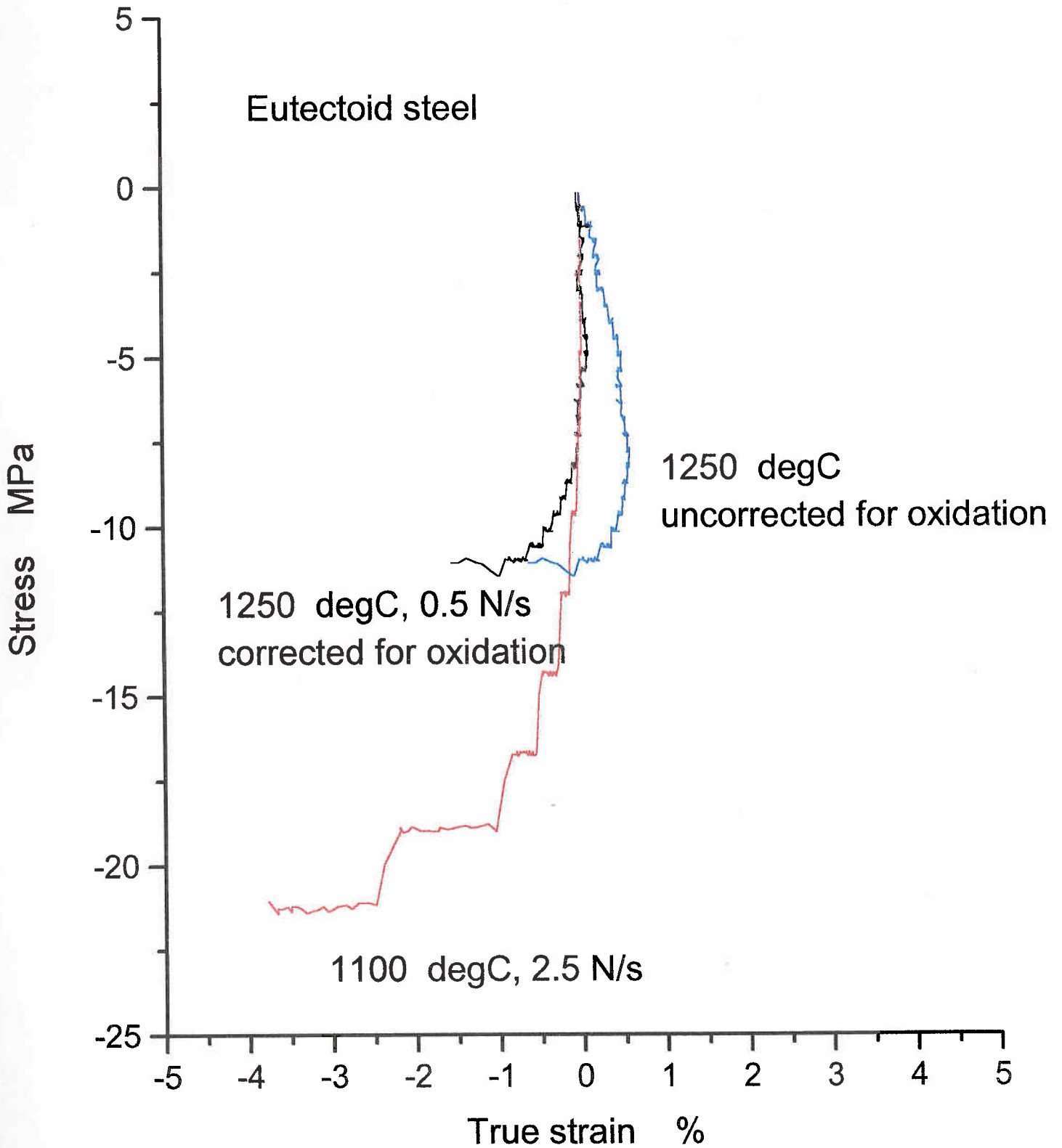


Fig 40 Compression stress/strain data for eutectoid steel at 1100 °C and 1250 °C, showing correction for oxidation.